Received August 4, 2021, accepted September 15, 2021, date of publication September 20, 2021,
date of current version September 29, 2021.

Digital Object Identifier 10.1109/ACCESS.2021.3114343

Security-Reliability Trade-Off Analysis for Rateless Codes-Based Relaying Protocols Using NOMA, Cooperative Jamming and Partial Relay Selection

DUY-HUNG HA[1], TRAN TRUNG DUY[2], (Member, IEEE), PHAM NGOC SON[3], THUONG LE-TIEN[4], (Member, IEEE), AND MIROSLAV VOZNAK[1], (Senior Member, IEEE)

[1]Faculty of Electrical Engineering and Computer Science, VSB—Technical University of Ostrava, 708 00 Ostrava, Czech Republic
[2]Posts and Telecommunications Institute of Technology, Ho Chi Minh City 700000, Vietnam
[3]Faculty of Electrical and Electronics Engineering, Ho Chi Minh City University of Technology and Education, Ho Chi Minh City 700000, Vietnam
[4]Ho Chi Minh City University of Technology, VNU-HCM, Ho Chi Minh City 700000, Vietnam

Corresponding author: Tran Trung Duy (trantrungduy@ptithcm.edu.vn)

This work was supported in part by Czech Ministry of Education, Youth and Sports under Project SP2021/25, and in part by the Large Infrastructures for Research, Experimental Development and Innovations Project "e-Infrastructure CZ" under Grant LM2018140.

ABSTRACT In this paper, we propose secure relaying transmission protocols using rateless codes, where a source sends encoded packets to two intended destinations via help of intermediate relays. Employing non-orthogonal multiple access, two encoded packets can be sent to the destinations at the same time. In addition, two partial relay selection methods are studied to enhance reliability of the data transmission at the first and second hops. For protecting the source-relay and relay-destination transmission against an eavesdropper, cooperative jamming technique is employed. Particularly, in the first phase of each data transmission cycle, the remaining relays (except the selected relay) are used to transmit artificial noise on the eavesdropper, and cooperate with the selected relay to cancel interference components. In the second phase, trusted nodes that are near the destinations are employed to play a role as the cooperative jammers. For a fair performance comparison, we design a simple transmit power allocation for the transmitter and jammer nodes at the first and second phases. We also propose an adaptive power allocation method, where fractions of the transmit power are appropriately allocated to the signals, relying on instantaneous channel gains between the selected relay and the destinations. This paper also derives exact closed-form formulas of outage probability and intercept probability over Rayleigh fading channel. All the performance analysis is then validated by Monte-Carlo simulations. The obtained results clearly show a trade-off between security and reliability that can be enhanced by optimally designing the system parameters.

INDEX TERMS Physical-layer security, rateless codes, NOMA, cooperative jamming, outage probability, intercept probability.

I. INTRODUCTION

The network security is an important topic object of different studies by scientific community as shown in many papers existing in literature [1]–[3]. Conventionally, complex data encryption methods at the upper layers are used to obtain the secure communication. Recently, researchers have proposed a new secure communication approach for wireless communications networks (WCNs), named physical-layer security (PLS) [4]–[7]. In PLS, physical channel parameters, such as link distances, channel state information (CSI) of data and/or eavesdropping channels, artificial noises (ANs), can be exploited to obtain security. For example, Reference [8] evaluates probability of positive secrecy capacity (PSC) for a dual-hop decode-and-forward (DF) relaying protocol, where secrecy capacity is difference between instantaneous channel capacity of the data and eavesdropping links. In addition, the transmitters in [8] including source and relay generate different code-books so that an eavesdropper cannot apply maximal ratio combining (MRC) as decoding the received

The associate editor coordinating the review of this manuscript and approving it for publication was Usama Mir.

signals. This randomize-and-forward (RaF) strategy is also used in [9] to enhance secure connectivity performance for cooperative wireless networks, with random appearance of eavesdroppers. In [10], [11], under impact of co-channel interference, various efficient relay selection methods are proposed to obtain better secrecy performance for DF and amplify-and-forward (AF) relaying protocols, respectively, in terms of PSC, secrecy outage probability (SOP) and average secrecy capacity (ASC). As shown in [10], [11], the relay selection methods provide higher channel capacity for the data links, which also leads to an increasing of secrecy capacity and the secrecy performance as well. To further enhance quality of the data channels, transmitting and receiving diversity techniques in multiple input multiple output (MIMO) relaying systems are proposed in [12], [13]. Published works [14], [15] analyze the secrecy performance of secondary networks operating on an underlay cognitive radio (UCR) mode, where transmit power of secondary transmitters is constrained by a maximal interference level required by a primary network. The key techniques considered in [14], [15] are cooperative relaying and transmit antenna selection (TAS), respectively. References [16], [17] concern with radio frequency energy harvesting (RF-EH) wiretap networks, where wireless transmitters have to harvest energy from wireless signals of power beacon stations for sending their data. Different with [8]- [17] that aim at evaluating the secrecy performance based on secrecy capacity, references [18]–[20] evaluate performance of the PLS schemes via two important metrics: outage probability (OP) at legitimate receivers and intercept probability (IP) at eavesdroppers. In addition, the results obtained in [18]–[20] present that there exists a trade-off between IP and OP, and this security-reliability trade-off (SRT) can be improved by applying efficient relay selection approaches.

The secrecy performance can be significantly enhanced by using cooperative jamming (CJ) technique [21], [22]. In CJ, one or multiple trusted nodes (called jammers) are assigned to transmit artificial noises (ANs) on eavesdroppers. Published literature [23] concerns with secrecy performance analysis of RF-EH wireless sensor networks (WSNs) employing CJ. Particularly, sensor nodes are powered by power stations deployed in the network, while a base station cooperates with a friendly jammer to discard ANs. In [24], the authors propose new zero-forcing beam-forming CJ methods for maximizing achievable secrecy rate, in presence of both passive and active eavesdroppers. In [25], [26], harvest-to-jam (HoT) strategies in PLS RF-EH environments are proposed, where jammer nodes first harvest wireless energy from ambient sources, and then use this energy to emit ANs. Published work [25] employs HoT to obtain security for dual-hop AF relaying protocols. HoT-aided DF relaying protocol using jammer selection methods is reported in [26]. Moreover, reference [26] uses the RaF strategy to confound eavesdroppers. The SRT performance of WCNs using CJ is investigated in [27]–[29]. In [27], user-pair selection is proposed to enhance reliability of the data transmission, while CJ is used for the secrecy enhancement purpose. In addition, imperfect interference cancellation at the legitimate destinations due to CSI estimation error is taken into account as calculating the performance. The authors of [28], [29] proposes opportunistic DF relay selection approaches for the SRT performance improvement in CJ-aided secure two-way relaying networks.

Non-orthogonal multiple access (NOMA) is a potential solution for next generation of WCNs due to much high spectral efficiency and low latency [30]. Unlike traditional orthogonal multiple access technologies such as FDMA, TDMA and CDMA; NOMA allows transmitters send multiple signals to intended receivers at the same frequency, time and code. To realize this, the transmitters linearly combine analog signals that are assigned with different transmit power levels. Then, the superposition signals are sent to the receivers. For extracting the desired data, successive interference cancellation (SIC) is adopted by the receivers. Recently, PLS-based protocols using NOMA have been gained much attention of researchers. Reference [31] studies the SOP performance of PLS MIMO-NOMA networks employing max-min TAS strategies, with presence of multiple colluding and non-colluding eavesdroppers. Published work [32] concerns with secrecy performance evaluation of AF and DF relaying in cooperative down-link NOMA networks including one central base station, two users, one single-antenna relay and one cell-edge eavesdropper. Three re-active relay selection methods are considered in [33] to obtain better secrecy performance for cooperative NOMA protocols, as compared with traditional relay selection methods. In [34], both secrecy and throughput performance of RF-EH internet-of-things (IoT) networks are evaluated. Particularly, a multi-antenna NOMA base station sends its data to IoT destinations via assistance of untrusted EH-AF relays. Like [34], a secure NOMA protocol with multiple untrusted EH-AF relays is introduced in [35]. Different with [34], multiple-antenna source and multiple-antenna destination in [35] can use maximal ratio transmission (MRT) and MRC techniques for transmitting and receiving the signals from the relays, respectively. Reference [36] considers a secure up-link NOMA transmission with CJ and jammer selection. In [37], [38], HoT is applied in cooperative NOMA protocols operating in the RF-EH environment. Reference [39] focuses on the SRT performance analysis for cooperative NOMA UCR networks, in terms of connection OP and SOP.

Due to simplicity and low latency, Rateless codes (RCs or Fountain codes) [40], [41] can be efficiently deployed in WCNs, especially WSNs, IoT, etc., in which wireless devices are limited in power, size, storage and processing capacity. Employing RCs, a transmitter can generate a limitless number of encoded packets which are sent its receivers. When the receivers collect a sufficient number of packets, the original data can be correctly recovered. As a result, the RCs receivers do not require the transmitter to re-send any specific packets that are received correctly. Therefore, RCs can reduce delay time from the feedback

as well as from the retransmission operation. Recently, PLS protocols adopting RCs have been reported in several publication such as [40]–[50] and references therein. For example, reference [40] shows that the original data is secure if a legitimate destination can gather enough number of packets before an eavesdropper. In [41], a DF relay is employed to forward the RCs packets to a destination, while a trusted relay plays a role as a jammer node to transmit noises on an eavesdropper. The authors in [41] evaluate quality-of-service violating probability (QVP) of the considered protocol, which is defined as probability of successful and secure receiving at the destination. In [42], four relay selection strategies are proposed to enhance reliability (OP) and/or security (IP) of the data transmission across two hops. Moreover, reference [42] studies efficient jammer selection algorithms to protect transmission of the RCs packets. Unlike [42], dual-hop DF relaying paradigm in [43] considered direct links from a source to a destination and to an eavesdropper. In addition, the authors in [43] propose a best relay selection method to minimize the QVP performance under a delay constraint. Reference [44] concerns with relay selection strategies for obtaining both reliability and security for RCs-based industrial IoT networks. The authors in [45] measure the IP and QVP performance of RCs-assisted MIMO systems adopting both TAS and CJ. In [46], the TAS and HoT techniques are applied in secure down-link transmission protocols using RCs, under joint impact of co-channel interference and hardware imperfection. In addition, the EH jammer in [46] has to collect RF energy from both base station and interference sources for the CJ operation. In [47]–[49], adaptively secure transmission protocols employing RCs and feedback channels are proposed. Published work [50] conducts IP and QVP performance analysis of unmanned aerial vehicle (UAV) systems with presence of ground full-duplex eavesdropper and jammer nodes.

This paper concerns with a RCs-based secure protocol using NOMA and CJ in dual-hop DF relaying networks. In the proposed protocol, a source uses NOMA to simultaneously send two RCs packets to two destinations via help of available intermediate relays. To protect the source-relay and relay-destination transmission under presence of an eavesdropper, CJ is deployed by the relays and employed jammers (nodes are near two destinations). We also consider two partial relay selection (PRS) methods to enhance the reliability of the packet transmission as well as to reduce the complexity implementation, as compared with full relay selection (FRS) ones [51], [52]. Different with the related works [40], [45], [46] which focus on RCs-aided one-hop secure transmission; our proposed scheme considers the dual-hop relaying one. Next, the main difference between our work and the related works [41]–[44] is the partial relay selection approaches and the CJ technique. Furthermore, the previous works [40]–[46] do not consider NOMA. The most related to our work is reference [53], in which NOMA is employed to directly send two RCs packets from a multiple-antenna source to multiple-antenna destination, using TAS/selection combining (SC) and TAS/MRC. However, the MIMO-NOMA paradigm in [53] only includes one destination, and does not exploit advantage of the CJ technique. Next, although reference [54] also studies the IP performance of secure relaying protocols employing RCs and CJ, but this work operates on cognitive environment, and a single-relay scheme is considered. Unlike [40]–[46], the relay in [54] does not forward each RCs packet to the destination. Instead, it attempts to recover the original data as soon as possible, so that it can replace the source to transmit the RCs packets to the destination.

To the best of our knowledge, there has been no published work related to the RCs-based secure transmission relaying protocol using NOMA, CJ and PRS. The proposed protocol can obtain better system performance, in terms of low delay time, high throughput, high spectral efficiency, low energy consumption, high reliability and high security. For reducing the delay time from end-to-end (also reducing the energy consumption, enhancing the throughput and spectral efficiency), the NOMA-based transmission is employed to send two encoded packets to two destinations at the same time, which also. To provide reliability for the transmission of the encoded packets, the PRS methods are used to obtain the spatial diversity at the first hop or the second hop. To obtain security for the original messages, the CJ technique is adopted at each hop to reduce quality of the eavesdropping links. In the following, new points and main contribution of this paper are summarized as follows:

- Firstly, we consider two partial relay selection methods. In the first one, the conventional PRS approach [55] is applied, where CSI between the source and relay nodes is used to select the best candidate. In the second one, we propose a new selection method, i.e., the relay is chosen by using CSI of the relay-destination links, and following a max-min criterion [55].
- Secondly, we consider a simple power allocation for the transmitters and the jammers. Moreover, to obtain performance fairness for the destinations, an adaptive power allocation approach for the transmitted signals is also proposed.
- Thirdly, exact closed-form expressions of OP and IP over Rayleigh fading channel are derived, and verified the accuracy by Monte Carlo simulations. Because the derived expressions are in closed-form, they can easily be used to evaluate and optimize the systems employing PRS-1 or PRS-2.
- Finally, the SRT performance of two proposed PRS protocols is investigated. In addition, performance comparison between our proposed protocols and the corresponding one without using CJ is also performed.

The rest of this paper is organized as follows. The system model of our proposed scenarios and their operation principle are shown in Section II. Section III aims at evaluating the OP and IP performance. Section IV verifies the analytical

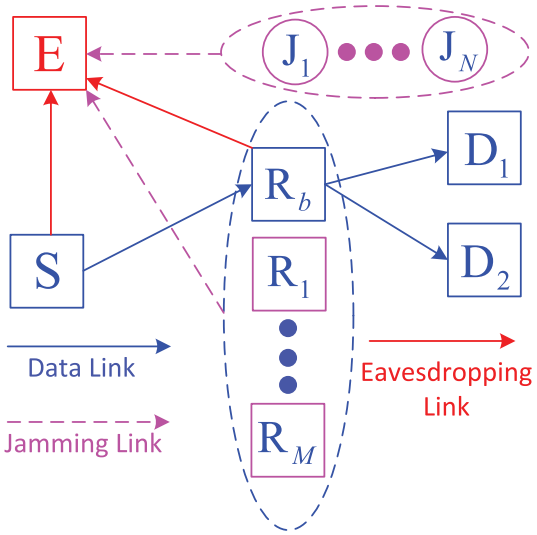

FIGURE 1. System model of the proposed RCs-based secure transmission protocol employing NOMA and CJ.

results via the simulated ones. Finally, useful conclusions and discussion are given in Section V.

II. SYSTEM MODEL

As illustrated in Fig. 1, a source node (S) wants to send messages T_1 and T_2 to two destination nodes D_1 and D_2, respectively. Due to far distances and obstacles, S cannot directly communicate with D_i, and hence the $S \rightarrow D_i$ communication is realized via help of available relays R_m, where $i = 1, 2$ and $m = 1, 2, \ldots, M, M+1$. Particularly, one of these relays is selected for the cooperation by using the PRS algorithms. For ease of presentation, in Fig. 1, we denote the chosen relay by $R_b \equiv R_{M+1}$ (the relay selection methods will be described in Sub-section 2.3). Also in the network, a passive eavesdropper (E) attempts to wiretap the confidential messages T_i. To protect the $S \rightarrow R_b$ transmission, the remaining relays (i.e., R_1, R_2,…,R_M) are employed to emit ANs on E. Also, the $R_b \rightarrow D$ secure transmission can be guaranteed by using friendly jammers J_n ($n = 1, 2, \ldots, N$). Moreover, for the interference cancellation at the receivers R_b and D_i, the jammers R_m and J_n are assumed to be close to R_b and D_i, respectively. In addition, to confuse E, the S and R_b nodes can cooperate with each other by using different code-books [8], [9]. It is also assumed that all the nodes are wireless single-antenna devices, and have to operate on a half-duplex (HD) mode. Our proposed protocol can be efficiently applied for WSNs, ad-hoc networks or IoT networks, in which there are a large number of nodes that can be employed for the cooperation in transmitting and jamming.

A. RATELESS CODES BASED DATA TRANSMISSION

Using RCs, the messages T_i ($i = 1, 2$) are divided into L_i short packets with equal length, respectively, which are used to generate the encoded packets. Next, S uses NOMA to send two encoded packets, e.g., $q_1[u]$ and $q_2[u]$, to D_1 and D_2, respectively, where $q_i[u]$ denotes the u-th packets of D_i, $u = 1, 2, 3, \ldots$. Due to the HD limitation, each $S \rightarrow R_b \rightarrow D_i$ transmission is split into two orthogonal time slots, i.e., S sends both $q_1[u]$ and $q_2[u]$ to R_b at the first time slot, and then R_b also uses NOMA to forward $q_1[u]$ and $q_2[u]$ (or only one packet, depends on the decoding status at R_b) to two destinations at the second time slot. To recover the original message T_i, D_i must collect at least H_i ($H_i \geq L_i$) encoded packets $q_i[u]$. Also, if E can obtain at least H_i packets, T_i is intercepted. Moreover, due to the delay constraint, the number of the $S \rightarrow R_b \rightarrow D_i$ transmission cycles is limited by $N_{\max}$, where $N_{\max} \geq H_1, N_{\max} \geq H_2$. Particularly, S will terminate its transmission after $N_{\max}$ transmission times. It is also noted that if the D_i and E nodes cannot receive enough H_i packets, T_i cannot be reconstructed successfully.

Remark 1: The proposed protocol can reduce the delay time, as compared with the corresponding protocol without using NOMA in which S has to send at least $2 \times N_{\max}$ RCs packets to two destinations. For ease of analysis and presentation, we can assume that $L_1 = L_2 = L$ and $H_1 = H_2 = H$. It is also noted that the proposed protocol can be easily extended to the corresponding ones with $L_1 \neq L_2$ ($H_1 \neq H_2$), as well as with higher number of the destinations.

B. CHANNEL MODEL

All the channels between two the nodes A and B are assumed to be block and flat Rayleigh fading, where $(A, B) \in \{S, R_m, J_n, D_i, E\}$. We denote h_{AB} and g_{AB} as channel coefficient and channel gain of the $A \rightarrow B$ links, respectively, where $g_{AB} = |h_{AB}|^2$. Therefore, g_{AB} is an exponential random variable (RV) whose cumulative distribution function (CDF) and probability density function (PDF) can be expressed, respectively as

$$\begin{aligned} F_{g_{AB}}(x) &= 1 - \exp(-\lambda_{AB} x), \\ f_{g_{AB}}(x) &= \lambda_{AB} \exp(-\lambda_{AB} x), \end{aligned} \tag{1}$$

where $F_{g_{AB}}(.)$ and $f_{g_{AB}}(.)$ refer to CDF and PDF of a RV g_{AB}, respectively, and λ_{AB} is modeled as [54], [55]

$$\lambda_{AB} = d_{AB}^{\xi}, \tag{2}$$

with d_{AB} is Euclid distance between A and B, and ξ ($2 \leq \xi \leq 8$) is path-loss exponent.

Remark 2: Due to block fading channel, g_{AB} is assumed to be unchanged during one transmission cycle, but independently varies over other ones. Next, since the relays are close together, we can assume that the distances between A and R_m are the same, i.e., $d_{SR_m} = d_{SR}$, $d_{R_m D_i} = d_{RD_i}$, $d_{R_m E} = d_{RE}$ ($\lambda_{SR_m} = \lambda_{SR}$, $\lambda_{R_m D_i} = \lambda_{RD_i}$, $\lambda_{R_m E} = \lambda_{RE}$) for all m and i. Similarly, it is also assumed that $\lambda_{J_n E} = \lambda_{JE}$ for all n when the J_n nodes are close together.

C. PARTIAL RELAY SELECTION METHODS

Before S starts the data transmission, R_b has to be selected for the cooperation. In the first relay selection approach, named PRS-1, the algorithm can be written, similarly to [55], as

$$g_{SR_b} = \max_{m=1,2,\ldots,M,M+1} \left(g_{SR_m}\right). \tag{3}$$

Equation (3) implies that R_b is the best candidate if the channel gain g_{SR_b} is highest. Moreover, g_{SR_b} is also a RV, and its CDF can be obtained as

$$\begin{aligned} F_{g_{SR_b}}(x) &= \Pr\left(\max_{m=1,2,\ldots,M,M+1} \left(g_{SR_m}\right) < x\right) \\ &= \left[F_{g_{SR_m}}(x)\right]^{M+1} \\ &= \left(1 - \exp\left(-\lambda_{SR} x\right)\right)^{M+1}. \end{aligned} \tag{4}$$

In the second relay selection approach, named PRS-2, we propose a max-min strategy to provide high channel quality for both the $R_b \rightarrow D_1$ and $R_b \rightarrow D_2$ links. In particular, by letting $\varphi_m = \min\left(g_{R_m D_1}, g_{R_m D_2}\right)$, the selection algorithm is expressed as follows:

$$\varphi_b = \max_{m=1,2,..,M+1} \left(\varphi_m\right). \tag{5}$$

Now, CDF of φ_m can be calculated as

$$\begin{aligned} F_{\varphi_m}(x) &= \Pr\left(\min\left(g_{R_m D_1}, g_{R_m D_2}\right) < x\right) \\ &= 1 - \left(1 - F_{g_{R_m D_1}}(x)\right)\left(1 - F_{g_{R_m D_2}}(x)\right) \\ &= 1 - \exp\left(-\Omega_{RD} x\right), \end{aligned} \tag{6}$$

where $\Omega_{RD} = \lambda_{SR} + \lambda_{RD}$.

According to (6), PDF of φ_m is given as

$$f_{\varphi_m}(x) = \Omega_{RD} \exp\left(-\Omega_{RD} x\right). \tag{7}$$

In addition, from (5) and (6), we obtain CDF of φ_b as

$$F_{\varphi_b}(x) = \left[F_{\varphi_m}(x)\right]^{M+1} = \left(1 - \exp\left(-\Omega_{RD} x\right)\right)^{M+1}. \tag{8}$$

Then, from (8), PDF of φ_b is shown as below:

$$\begin{aligned} f_{\varphi_b}(x) &= (M+1)\,\Omega_{RD} \exp\left(-\Omega_{RD} x\right)\left(1 - \exp\left(-\Omega_{RD} x\right)\right)^M \\ &= \sum_{p=0}^{M} (-1)^p C_M^p\,(M+1)\Omega_{RD} \exp\left(-(p+1)\,\Omega_{RD} x\right), \end{aligned} \tag{9}$$

where C_b^a denotes a binomial coefficient, i.e.,

$$C_b^a = \frac{b!}{a!\,(b-a)!}. \tag{10}$$

Remark 3: Although PRS-1 can enhance reliability of the data transmission at the first hop, the data transmission at the second hop may be not reliable when the relay-destination distances are far. On the contrary, PRS-2 can perform well when the relays are far the destinations because the relay selection is realized at the second hop. However, the performance of PRS-2 is not good when the relays are not close to the source. This paper only studies the PRS methods because their implementation is much simpler than the FRS one [55]. Indeed, the FRS method requires CSI of both the hops, which takes much time and energy due to a high synchronization and a complex CSI estimation. In addition, when the number of relays increases, the delay time and the energy consumption significantly increase. Therefore, the FRS method may be not suitable for the energy-constrained wireless networks such as WSNs and IoT. On the contrary, PRS-1 and PRS-2 only use CSI at the first hop and the second hop for selecting the best relay, respectively. It is worth noting that the partial CSI can be easily obtained via control messages generated at set-up phases and maintenance phases.

D. TRANSMIT POWER FORMULATION

For a fair performance comparison between the scenarios using different number of jammers, the total transmit power of the transmitter and jammer nodes, at the first and second time slots, is fixed by P_{tot}, i.e.,

$$\begin{cases} P_S + \sum_{m=1}^{M} P_{R_m} = P_{tot} \\ P_{R_b} + \sum_{n=1}^{N} P_{J_n} = P_{tot} \end{cases} \tag{11}$$

In (11), P_A is transmit power of the node A ($A \in \{S, R_m, R_b, J_n\}$). We then consider a simple power allocation approach, where the transmit power of the jammer nodes is equally allocated, i.e.,

$$\begin{cases} P_S = \mu P_{tot}, P_{R_m} = \dfrac{1-\mu}{M} P_{tot} \\ P_{R_b} = \mu P_{tot}, P_{J_n} = \dfrac{1-\mu}{N} P_{tot}. \end{cases} \tag{12}$$

Remark 4: In (12), the factor μ is a pre-determined system parameter, where $0 < \mu \leq 1$. It is worth noting that the CJ model with multiple jammer nodes is a generalized model, and this power allocation method guarantees an equal power consumption among the considered scenarios. Moreover, if the CJ technique is not used, μ is set to 1, and we have

$$\begin{cases} P_S = P_{tot}, P_{R_m} = 0 \\ P_{R_b} = P_{tot}, P_{J_n} = 0. \end{cases} \tag{13}$$

E. TRANSMISSION OF ENCODED PACKETS

This sub-section presents the transmission of each encoded packet which is split into two orthogonal time slots. Assume that S sends the packets $q_1[u]$ and $q_2[u]$ to D_1 and D_2, respectively. Let us denote $\mathcal{Q}$ (symbols) as length of $q_1[u]$ and $q_2[u]$. According to the principle of NOMA, S linearly combines modulated signals of $q_1[u]$ and $q_2[u]$ as

$$x_+[v] = \sqrt{a_1 P_S} x_1[v] + \sqrt{a_2 P_S} x_2[v], \tag{14}$$

where $x_1[v]$ and $x_2[v]$ ($v = 1, 2, \ldots, \mathcal{Q}$) are modulated signals of the v-th symbol of $q_1[u]$ and $q_2[u]$, respectively, $a_1 P_S$ and $a_2 P_S$ are transmit power allocated to $x_1[v]$ and $x_2[v]$, respectively.

Remark 5: In NOMA, it is commonly assumed that one of two destinations, (e.g., D_1) has better channel to the transmitters, (e.g., D_1 (strong user) is near R_b, and D_2 (week user) is far R_b). Therefore, during the data transmission, the factors a_1 and a_2 are always assigned by $0 < a_1 < a_2 < 1$ and $a_1 + a_2 = 1$ (see [31], [33], [34]). However, this method can lead to a performance unfairness between D_1 and D_2. In non-infrastructure networks such as WSNs, due to the limited transmit power, radio range of the wireless nodes is short. If all the nodes in this paper are sensors, the distances between the relays and two destinations, i.e., d_{RD_1} and d_{RD_2}, may be not much different. In this case, the conventional NOMA transmission models in [31], [33], [34] may not be applied. In addition, motivated by obtaining the performance fairness for two destinations, we propose an adaptive power allocation strategy as follows:

$$\begin{cases} a_1 = \alpha, a_2 = \beta, & \text{if } g_{\mathrm{R}_b\mathrm{D}_1} \le g_{\mathrm{R}_b\mathrm{D}_2} \\ a_1 = \beta, a_2 = \alpha, & \text{if } g_{\mathrm{R}_b\mathrm{D}_1} > g_{\mathrm{R}_b\mathrm{D}_2}. \end{cases} \tag{15}$$

where $0 \le \beta < \alpha \le 1$ and $\alpha + \beta = 1$.

Note that the factors α and β are pre-designed system parameters. We also observe from (15) that when the $R_b \to D_2$ link is better than the $R_b \to D_1$ one, more transmit power should be allocated to the modulated signals of $q_1[u]$, and vice verse. Now, we consider the following two cases:

Case 1: $a_1 = \alpha,\ a_2 = \beta\ \left(g_{\mathrm{R}_b\mathrm{D}_1} \le g_{\mathrm{R}_b\mathrm{D}_2}\right)$

In this case, the superposition signal in (14) becomes

$$x_+[v] = \sqrt{\alpha P_{\mathrm{S}}}x_1[v] + \sqrt{\beta P_{\mathrm{S}}}x_2[v]. \tag{16}$$

Recalling that during the $S \to R_b$ transmission, the remaining relays emit ANs, and hence the signals received at R_b and E can be expressed, respectively as

$$\begin{aligned} y_{\mathrm{SR}_b}[v] &= h_{\mathrm{SR}_b}x_+[v] + \sum_{m=1}^{M} P_{\mathrm{R}_m}h_{\mathrm{R}_m\mathrm{R}_b}z_m[v] + \varepsilon_{\mathrm{R}_b}[v], \\ y_{\mathrm{SE}}[v] &= h_{\mathrm{SE}}x_+[v] + \sum_{m=1}^{M} P_{\mathrm{R}_m}h_{\mathrm{R}_m\mathrm{E}}z_m[v] + \varepsilon_{\mathrm{E}}[v]. \end{aligned} \tag{17}$$

In (17), $z_m[v]$ is the v-th jamming signal generated by R_m, and $\varepsilon_{\mathrm{B}}[.]$ denotes Additive White Gaussian Noise (AWGN) at the receiver B, where $\mathrm{B} \in \{\mathrm{R}_b, \mathrm{E}\}$. Without loss of generality, we assume that all the AWGNs have zero mean and variance of σ_0^2. Because $z_m[v]$ is known by R_b, the interference components $P_{\mathrm{R}_m}h_{\mathrm{R}_m\mathrm{R}_b}z_m[v]$ can be removed from the received signal $y_{\mathrm{SR}_b}[v]$. Hence, after the interference cancellation, $y_{\mathrm{SR}_b}[v]$ becomes

$$\begin{aligned} y^*_{\mathrm{SR}_b}[v] &= h_{\mathrm{SR}_b}x_+[v] + \varepsilon_{\mathrm{R}_b}[v] \\ &= \sqrt{\alpha P_{\mathrm{S}}}h_{\mathrm{SR}_b}x_1[v] + \sqrt{\beta P_{\mathrm{S}}}h_{\mathrm{SR}_b}x_2[v] + \varepsilon_{\mathrm{R}_b}[v]. \end{aligned} \tag{18}$$

Next, R_b first decodes $x_1[u]$, and from (12) and (18), the effective signal-to-noise ratio (SNR) can be calculated as

$$\gamma^{\mathrm{C1}}_{\mathrm{SR}_b,x_1} = \frac{\alpha P_{\mathrm{S}}g_{\mathrm{SR}_b}}{\beta P_{\mathrm{S}}g_{\mathrm{SR}_b} + \sigma_0^2} = \frac{\alpha\mu\Delta g_{\mathrm{SR}_b}}{\beta\mu\Delta g_{\mathrm{SR}_b} + 1}, \tag{19}$$

where $\Delta = P_{\mathrm{tot}}/\sigma_0^2$ denotes the transmit SNR.

If R_b can correctly decode $x_1[v]$, after removing the component $\sqrt{\alpha P_{\mathrm{S}}}h_{\mathrm{SR}_b}x_1[v]$, $y^*_{\mathrm{SR}_b}[v]$ becomes $y^{**}_{\mathrm{SR}_b}$ as

$$y^{**}_{\mathrm{SR}_b}[v] = \sqrt{\beta P_{\mathrm{S}}}h_{\mathrm{SR}_b}x_2[v] + \varepsilon_{\mathrm{R}_b}[v]. \tag{20}$$

From (20), the obtained SNR for decoding $x_2[v]$ is

$$\gamma^{\mathrm{C1}}_{\mathrm{SR}_b,x_2} = \frac{\beta P_{\mathrm{S}}g_{\mathrm{SR}_b}}{\sigma_0^2} = \beta\mu\Delta g_{\mathrm{SR}_b}. \tag{21}$$

With the same manner as R_b, E first decodes $x_1[v]$, and then applies SIC to decode $x_2[v]$. On the other hand, because E cannot remove ANs caused by the relays, the signal-to-interference-plus-noise ratios (SINRs) obtained at E for decoding $x_1[v]$ and $x_2[v]$ can be respectively computed, based on (17), as

$$\begin{aligned} \gamma^{\mathrm{C1}}_{\mathrm{SE},x_1} &= \frac{\alpha\mu\Delta g_{\mathrm{SE}}}{\beta\mu\Delta g_{\mathrm{SE}} + \Lambda_1\sum_{m=1}^{M} g_{\mathrm{R}_m\mathrm{E}} + 1}, \\ \gamma^{\mathrm{C1}}_{\mathrm{SE},x_2} &= \frac{\beta\mu\Delta g_{\mathrm{SE}}}{\Lambda_1\sum_{m=1}^{M} g_{\mathrm{R}_m\mathrm{E}} + 1}, \end{aligned} \tag{22}$$

where $\Lambda_1 = P_{\mathrm{R}_m}/\sigma_0^2 = (1-\mu)\Delta/M$.

Remark 6: Assume that that the signals $x_i[v]$ can be successfully decoded by the receiver B, if the obtained SNR (SINR) is higher than a pre-determined threshold, i.e., γ_{th}, where $\mathrm{B} \in \{\mathrm{R}_b, \mathrm{E}, \mathrm{D}_i\}$. Otherwise, $x_i[v]$ cannot be correctly decoded by B. Moreover, because the channel coefficients do not change during the data transmission, the successful decoding probability of $x_i[v]$ is equivalent to that of $q_i[u]$.

In the following, we present the data transmission between R_b and D_i in the second time slot in three sub-cases as follows: i) R_b can decode both $q_1[u]$ and $q_2[u]$ successfully ($\gamma^{\mathrm{C1}}_{\mathrm{R}_b,x_1} \ge \gamma_{\mathrm{th}}$, $\gamma^{\mathrm{C1}}_{\mathrm{R}_b,x_2} \ge \gamma_{\mathrm{th}}$); ii) R_b only decodes $q_1[u]$ successfully ($\gamma^{\mathrm{C1}}_{\mathrm{R}_b,x_1} \ge \gamma_{\mathrm{th}}$, $\gamma^{\mathrm{C1}}_{\mathrm{R}_b,x_2} < \gamma_{\mathrm{th}}$); iii) R_b cannot decode $q_1[u]$ successfully ($\gamma^{\mathrm{C1}}_{\mathrm{R}_b,x_1} < \gamma_{\mathrm{th}}$, and $q_2[u]$ is also unsuccessfully decoded because R_b cannot remove the components including $x_1[v]$).

Case 1.1: *Both $q_1[u]$ and $q_2[u]$ are correctly decoded*

In this sub-case, R_b combines $q_1[u]$ and $q_2[u]$ as S did in the first time slot, i.e., $x_+[v] = \sqrt{\alpha P_{\mathrm{R}_b}}x_1[v] + \sqrt{\beta P_{\mathrm{R}_b}}x_2[v]$. Next, it sends $x_+[v]$ to D_i in the second time slot. Under the impact of ANs from J_n, the signals at D_i and E, can be expressed, respectively as

$$\begin{aligned} y_{\mathrm{R}_b\mathrm{D}_i}[v] &= h_{\mathrm{R}_b\mathrm{D}_i}x_+[v] + \sum_{n=1}^{N} P_{\mathrm{J}_n}h_{\mathrm{J}_n\mathrm{D}_i}l_n[v] + \varepsilon_{\mathrm{D}_i}[v], \\ y_{\mathrm{R}_b\mathrm{E}}[v] &= h_{\mathrm{R}_b\mathrm{E}}x_+[v] + \sum_{n=1}^{N} P_{\mathrm{J}_n}h_{\mathrm{J}_n\mathrm{E}}l_n[v] + \varepsilon_{\mathrm{E}}[v], \end{aligned} \tag{23}$$

where $l_n[v]$ is the v-th jamming signal of J_n, and $\varepsilon_{\mathrm{D}_i}[v]$ is AWGN at D_i. Then, after removing the interference components, $y_{\mathrm{R}_b\mathrm{D}_i}[v]$ in (23) can be written as

$$y^*_{\mathrm{R}_b\mathrm{D}_i}[v] = \sqrt{\alpha P_{\mathrm{R}_b}}h_{\mathrm{R}_b\mathrm{D}_i}x_1[v] + \sqrt{\beta P_{\mathrm{R}_b}}h_{\mathrm{R}_b\mathrm{D}_i}x_2[v] + \varepsilon_{\mathrm{D}_i}[v]. \tag{24}$$

Since D_1 directly decodes $x_1[v]$, based on (12) and (24), the effective SNR can be formulated as

$$\gamma^{\text{C1.1}}_{\text{R}_b\text{D}_1,x_1} = \frac{\alpha\mu\Delta g_{\text{R}_b\text{D}_1}}{\beta\mu\Delta g_{\text{R}_b\text{D}_1}+1}. \quad (25)$$

For D_2, $x_1[v]$ is first decoded, and then subtracted before decoding $x_2[v]$. Hence, the effective SNRs, with respect to $x_1[v]$ and $x_2[v]$, are respectively obtained as

$$\gamma^{\text{C1.1}}_{\text{R}_b\text{D}_2,x_1} = \frac{\alpha\mu\Delta g_{\text{R}_b\text{D}_2}}{\beta\mu\Delta g_{\text{R}_b\text{D}_2}+1}, \gamma^{\text{C1.1}}_{\text{R}_b\text{D}_2,x_2} = \beta\mu\Delta g_{\text{R}_b\text{D}_2}. \quad (26)$$

For E; since the interference cancellation cannot be carried out, based on (12) and (23), the obtained SINRs for decoding $x_1[v]$ and $x_2[v]$ can be given, respectively as

$$\gamma^{\text{C1.1}}_{\text{R}_b\text{E},x_1} = \frac{\alpha\mu\Delta g_{\text{R}_b\text{E}}}{\beta\mu\Delta g_{\text{R}_b\text{E}}+\Lambda_2\sum_{n=1}^{N} g_{\text{J}_n\text{E}}+1},$$
$$\gamma^{\text{C1.1}}_{\text{R}_b\text{E},x_2} = \frac{\beta\mu\Delta g_{\text{R}_b\text{E}}}{\Lambda_2\sum_{n=1}^{N} g_{\text{J}_n\text{E}}+1}, \quad (27)$$

where $\Lambda_2 = P_{\text{J}_n}/\sigma_0^2 = (1-\mu)\Delta/N$.

Case 1.2: *Only $q_1[u]$ is correctly decoded*

In this sub-case, R_b only sends $q_1[u]$ to D_1, using the transmit power P_{R_b}. Hence, the signals received at D_1 and E at the second time slot can be expressed, respectively as

$$y_{\text{R}_b\text{D}_1}[v] = \sqrt{P_{\text{R}_b}}h_{\text{R}_b\text{D}_1}x_1[v] + \sum_{n=1}^{N} P_{\text{J}_n}h_{\text{J}_n\text{D}_1}l_n[v] + \varepsilon_{\text{D}_1}[v],$$
$$y_{\text{R}_b\text{E}}[v] = \sqrt{P_{\text{R}_b}}h_{\text{R}_b\text{E}}x_1[v] + \sum_{n=1}^{N} P_{\text{J}_n}h_{\text{J}_n\text{E}}l_n[v] + \varepsilon_{\text{E}}[v]. \quad (28)$$

Also, only D_1 can perform the AN cancellation, and hence SNR at D_1 and SINR at E can be formulated, respectively as

$$\gamma^{\text{C1.2}}_{\text{R}_b\text{D}_1,x_1} = \mu\Delta g_{\text{R}_b\text{D}_1}, \gamma^{\text{C1.2}}_{\text{R}_b\text{E},x_1} = \frac{\mu\Delta g_{\text{R}_b\text{E}}}{\Lambda_2\sum_{n=1}^{N} g_{\text{J}_n\text{E}}+1}. \quad (29)$$

Case 1.3: *$q_1[u]$ ($q_2[u]$) is unsuccessfully decoded*

In this sub-case, R_b cannot transmit any encoded packet to the destinations at the second time slot.

Case 2: $a_1 = \beta,\ a_2 = \alpha\ \left(g_{\text{R}_b\text{D}_1} > g_{\text{R}_b\text{D}_2}\right)$

In Case 2, the modulated signals of $q_2[u]$ are allocated with higher transmit power, i.e., $x_+[v] = \sqrt{\alpha P_{\text{A}}}x_2[v] + \sqrt{\beta P_{\text{A}}}x_1[v]$, where $A \in \{\text{S}, \text{R}_b\}$. Therefore, $x_2[v]$ is first detected, and then removed by the receiver B before detecting $x_1[v]$, where $\text{B} \in \{\text{R}_b, \text{D}_i, \text{E}\}$. Similar to Case 1, we can formulate SNRs at R_b and SINRs at E, with respect to $x_2[v]$ and $x_1[v]$, respectively as

$$\gamma^{\text{C2}}_{\text{SR}_b,x_2} = \frac{\alpha\mu\Delta g_{\text{SR}_b}}{\beta\mu\Delta g_{\text{SR}_b}+1}, \gamma^{\text{C2}}_{\text{SR}_b,x_1} = \beta\mu\Delta g_{\text{SR}_b},$$
$$\gamma^{\text{C2}}_{\text{SE},x_2} = \frac{\alpha\mu\Delta g_{\text{SE}}}{\beta\mu\Delta g_{\text{SE}}+\Lambda_1\sum_{m=1}^{M} g_{\text{R}_m\text{E}}+1},$$
$$\gamma^{\text{C2}}_{\text{SE},x_1} = \frac{\beta\mu\Delta g_{\text{SE}}}{\Lambda_1\sum_{m=1}^{M} g_{\text{R}_m\text{E}}+1}. \quad (30)$$

Case 2.1: *Both $q_1[u]$ and $q_2[u]$ are correctly decoded*

Similarly, SNRs received at D_1 are given, respectively as

$$\gamma^{\text{C2.1}}_{\text{R}_b\text{D}_1,x_2} = \frac{\alpha\mu\Delta g_{\text{R}_b\text{D}_1}}{\beta\mu\Delta g_{\text{R}_b\text{D}_1}+1}, \gamma^{\text{C2.1}}_{\text{R}_b\text{D}_1,x_1} = \beta\mu\Delta g_{\text{R}_b\text{D}_1}. \quad (31)$$

At D_2, $q_2[u]$ is directly detected by treating $q_1[u]$ as noises, and SNR is computed as

$$\gamma^{\text{C2.1}}_{\text{R}_b\text{D}_2,x_2} = \frac{\alpha\mu\Delta g_{\text{R}_b\text{D}_2}}{\beta\mu\Delta g_{\text{R}_b\text{D}_2}+1}. \quad (32)$$

For E, we can express the obtained SINRs as follows:

$$\gamma^{\text{C2.1}}_{\text{R}_b\text{E},x_2} = \frac{\alpha\mu\Delta g_{\text{R}_b\text{E}}}{\beta\mu\Delta g_{\text{R}_b\text{E}}+\Lambda_2\sum_{n=1}^{N} g_{\text{J}_n\text{E}}+1},$$
$$\gamma^{\text{C2.1}}_{\text{R}_b\text{E},x_1} = \frac{\beta\mu\Delta g_{\text{R}_b\text{E}}}{\Lambda_2\sum_{n=1}^{N} g_{\text{J}_n\text{E}}+1}. \quad (33)$$

Case 2.2: *Only $q_2[u]$ is correctly decoded*

In this sub-case, R_b sends $q_2[u]$ to D_2. Similarly, SNR at D_2 and SINR at E can be formulated, respectively as

$$\gamma^{\text{C2.2}}_{\text{R}_b\text{D}_2,x_2} = \mu\Delta g_{\text{R}_b\text{D}_2}, \gamma^{\text{C2.2}}_{\text{R}_b\text{E},x_2} = \frac{\mu\Delta g_{\text{R}_b\text{E}}}{\Lambda_2\sum_{n=1}^{N} g_{\text{J}_n\text{E}}+1}. \quad (34)$$

Case 2.3: *$q_2[u]$ ($q_1[u]$) is unsuccessfully decoded*

Similar to Case 1.3, there is no data transmission at the second time slot.

III. PERFORMANCE EVALUATION

This section focus on evaluating OP and IP of the methods PRS-1 and PRS-2. At first, we consider the probability that one encoded packet can be correctly received by D_i and E in the PRS-i method (i=1,2).

A. PRS-1 METHOD

Theorem 1: The probability that one encoded packet is successfully reached to D_i in PRS-1 can be expressed by an exact closed-form expression as shown in (35), as shown at the bottom of the next page, where

$$\omega_{1,\text{th}} = \frac{\gamma_{\text{th}}}{\mu\Delta(\alpha-\beta\gamma_{\text{th}})}, \omega_{2,\text{th}} = \frac{\gamma_{\text{th}}}{\mu\Delta\beta}, \omega_{3,\text{th}} = \frac{\gamma_{\text{th}}}{\mu\Delta}. \quad (36)$$

Proof: See the proof in Appendix A.

Remark 7: As discussed in [53], to obtain high SNR for the priority signal $x_1[v]$ in Case 1, and for the priority signal $x_2[v]$ in Case 2 under impact of the interference from the remaining signal, the factors α and β should be designed as

$$\alpha > \frac{1+\gamma_{\text{th}}}{2+\gamma_{\text{th}}} \text{ or } \beta < \frac{1}{2+\gamma_{\text{th}}}. \quad (37)$$

According to (37), it is straightforward that $\omega_{2,\text{th}} > \omega_{1,\text{th}} > 0$. It is also worth noting that the values of α and β are satisfied (37) in all the derivations in Section III.

Theorem 2: The probability that the packet $q_i[u]$ is correctly decoded by E in PRS-1 can be given by an exact closed-form formula as in (38), as shown at the bottom of the page, where

$$\omega_{4,\text{th}} = \frac{(1-\mu)\,\gamma_{\text{th}}}{M\mu\,(\alpha-\beta\gamma_{\text{th}})}, \quad \omega_{5,\text{th}} = \frac{(1-\mu)\,\gamma_{\text{th}}}{N\mu\,(\alpha-\beta\gamma_{\text{th}})},$$
$$\omega_{6,\text{th}} = \frac{(1-\mu)\,\gamma_{\text{th}}}{N\mu}, \quad \omega_{7,\text{th}} = \frac{(1-\mu)\,\gamma_{\text{th}}}{M\mu\beta},$$
$$\omega_{8,\text{th}} = \frac{(1-\mu)\,\gamma_{\text{th}}}{N\mu\beta}, \text{ and } \begin{cases} j=2, & \text{if } i=1 \\ j=1, & \text{if } i=2. \end{cases} \tag{39}$$

Proof: See the proof in Appendix B.

Next, we evaluate $\theta_{\text{T}i}^{\text{PRS}-i}$ at high transmit SNR values, as in Corollary 1 below.

Corollary 1: At high transmit SNR, i.e., $\Delta \to +\infty$, $\theta_{\text{T}i}^{\text{PRS}-1}$ can be approximated by (40), as shown at the bottom of the next page.

Proof: It is straightforward that $\omega_{1,\text{th}}, \omega_{2,\text{th}}, \omega_{3,\text{th}}, \overset{\Delta\to+\infty}{\approx} 0$. Hence, substituting $\omega_{1,\text{th}} = \omega_{2,\text{th}} = \omega_{3,\text{th}} = 0$ into (38), and after some mathematical manipulation, we obtain (40). As observed, $\theta_{\text{T}i}^{\text{PRS}-1}$ at high Δ values does not depend on Δ.

B. PRS-2 METHOD

Theorem 3: The probability that one encoded packet is successfully reached to D_i in PRS-2 can be expressed as in (41), as shown at the bottom of the next page, where $\begin{cases} j=2, & \text{if } i=1 \\ j=1, & \text{if } i=2 \end{cases}$.

Proof: See the proof in Appendix C.

Theorem 4: The probability that $q_i[u]$ is correctly decoded by E in PRS-2 is given by (42), as shown at the bottom of the next page, where $\begin{cases} j=2, & \text{if } i=1 \\ j=1, & \text{if } i=2 \end{cases}$.

Proof: See the proof in Appendix D.

Corollary 2: At high transmit SNR, $\theta_{\text{T}i}^{\text{PRS}-2}$ can be approximated by (43), as shown at the bottom of the next page.

Proof: Substituting $\omega_{1,\text{th}} = \omega_{2,\text{th}} = \omega_{3,\text{th}} = 0$ into (42), we can obtain (43). Also, $\theta_{\text{T}i}^{\text{PRS}-2}$ at high Δ regime does not depend on Δ. Moreover, it is worth pointing out from (40) and (43) that $\theta_{\text{T}i}^{\text{PRS}-1}$ and $\theta_{\text{T}i}^{\text{PRS}-2}$ at high Δ values are the same.

$$\begin{aligned}\theta_{\text{Di}}^{\text{PRS}-1} = {} & \left[1-\left(1-\exp\left(-\lambda_{\text{SR}}\omega_{2,\text{th}}\right)\right)^{M+1}\right]\frac{\lambda_{\text{RD}_i}}{\Omega_{\text{RD}}}\exp\left(-\Omega_{\text{RD}}\omega_{1,\text{th}}\right) \\ & + \left[\left(1-\exp\left(-\lambda_{\text{SR}}\omega_{2,\text{th}}\right)\right)^{M+1} - \left(1-\exp\left(-\lambda_{\text{SR}}\omega_{1,\text{th}}\right)\right)^{M+1}\right]\frac{\lambda_{\text{RD}_i}}{\Omega_{\text{RD}}}\exp\left(-\Omega_{\text{RD}}\omega_{3,\text{th}}\right) \\ & + \left[1-\left(1-\exp\left(-\lambda_{\text{SR}}\omega_{2,\text{th}}\right)\right)^{M+1}\right]\left(\exp\left(-\lambda_{\text{RD}_i}\omega_{2,\text{th}}\right) - \frac{\lambda_{\text{RD}_i}}{\Omega_{\text{RD}}}\exp\left(-\Omega_{\text{RD}}\omega_{2,\text{th}}\right)\right). \end{aligned} \tag{35}$$

$$\begin{aligned}\theta_{\text{Ti}}^{\text{PRS}-1} = {} & \frac{\lambda_{\text{RD}_i}}{\Omega_{\text{RD}}}\left(\frac{\lambda_{\text{RE}}}{\lambda_{\text{RE}}+\lambda_{\text{SE}}\omega_{4,\text{th}}}\right)^{M}\exp\left(-\lambda_{\text{SE}}\omega_{1,\text{th}}\right) + \frac{\lambda_{\text{RD}_j}}{\Omega_{\text{RD}}}\left(\frac{\lambda_{\text{RE}}}{\lambda_{\text{RE}}+\lambda_{\text{SE}}\omega_{7,\text{th}}}\right)^{M}\exp\left(-\lambda_{\text{SE}}\omega_{2,\text{th}}\right) \\ & + \frac{\lambda_{\text{RD}_i}}{\Omega_{\text{RD}}}\left[1-\left(\frac{\lambda_{\text{RE}}}{\lambda_{\text{RE}}+\lambda_{\text{SE}}\omega_{4,\text{th}}}\right)^{M}\exp\left(-\lambda_{\text{SE}}\omega_{1,\text{th}}\right)\right]\left[1-\left(1-\exp\left(-\lambda_{\text{SR}}\omega_{2,\text{th}}\right)\right)^{M+1}\right] \\ & \times\left(\frac{\lambda_{\text{JE}}}{\lambda_{\text{JE}}+\lambda_{\text{RE}}\omega_{5,\text{th}}}\right)^{N}\exp\left(-\lambda_{\text{RE}}\omega_{1,\text{th}}\right) \\ & + \frac{\lambda_{\text{RD}_i}}{\Omega_{\text{RD}}}\left[1-\left(\frac{\lambda_{\text{RE}}}{\lambda_{\text{RE}}+\lambda_{\text{SE}}\omega_{4,\text{th}}}\right)^{M}\exp\left(-\lambda_{\text{SE}}\omega_{1,\text{th}}\right)\right]\left[\left(1-\exp\left(-\lambda_{\text{SR}}\omega_{2,\text{th}}\right)\right)^{M+1} - \left(1-\exp\left(-\lambda_{\text{SR}}\omega_{1,\text{th}}\right)\right)^{M+1}\right] \\ & \times\left(\frac{\lambda_{\text{JE}}}{\lambda_{\text{JE}}+\lambda_{\text{RE}}\omega_{6,\text{th}}}\right)^{N}\exp\left(-\lambda_{\text{RE}}\omega_{3,\text{th}}\right) \\ & + \frac{\lambda_{\text{RD}_j}}{\Omega_{\text{RD}}}\left[\left(\frac{\lambda_{\text{RE}}}{\lambda_{\text{RE}}+\lambda_{\text{SE}}\omega_{4,\text{th}}}\right)^{M}\exp\left(-\lambda_{\text{SE}}\omega_{1,\text{th}}\right) - \left(\frac{\lambda_{\text{RE}}}{\lambda_{\text{RE}}+\lambda_{\text{SE}}\omega_{7,\text{th}}}\right)^{M}\exp\left(-\lambda_{\text{SE}}\omega_{2,\text{th}}\right)\right] \\ & \times\left[1-\left(1-\exp\left(-\lambda_{\text{SR}}\omega_{2,\text{th}}\right)\right)^{M+1}\right]\left(\frac{\lambda_{\text{JE}}}{\lambda_{\text{JE}}+\lambda_{\text{RE}}\omega_{8,\text{th}}}\right)^{N}\exp\left(-\lambda_{\text{RE}}\omega_{2,\text{th}}\right) \\ & + \frac{\lambda_{\text{RD}_j}}{\Omega_{\text{RD}}}\left[1-\left(\frac{\lambda_{\text{RE}}}{\lambda_{\text{RE}}+\lambda_{\text{SE}}\omega_{4,\text{th}}}\right)^{M}\exp\left(-\lambda_{\text{SE}}\omega_{1,\text{th}}\right)\right]\left[1-\left(1-\exp\left(-\lambda_{\text{SR}}\omega_{2,\text{th}}\right)\right)^{M+1}\right] \\ & \times\left(\frac{\lambda_{\text{JE}}}{\lambda_{\text{JE}}+\lambda_{\text{RE}}\omega_{8,\text{th}}}\right)^{N}\exp\left(-\lambda_{\text{RE}}\omega_{2,\text{th}}\right). \end{aligned} \tag{38}$$

C. ANALYSIS OF OP AND IP

Firstly, OP at D_i in PRS-i can be exactly computed as

$$\mathrm{OP}_{\mathrm{D}i}^{\mathrm{PRS}-i} = \sum_{N=0}^{H-1} C_{N_{\max}}^{N} \left(\theta_{\mathrm{Di}}^{\mathrm{PRS}-i}\right)^{N} \left(1-\theta_{\mathrm{Di}}^{\mathrm{PRS}-i}\right)^{N_{\max}-N}, \quad (44)$$

where $\theta_{\mathrm{D}i}^{\mathrm{PRS}-i}$ is given in (35) and (41).

In (44), because D_i only collects N ($0 \le N < H$) packets after S stops the transmission, it cannot recover the original message T_i. It is worth noting that probability that D_i in PRS-i incorrectly receives the packet $q_i[u]$ is $1-\theta_{\mathrm{Di}}^{\mathrm{PRS-i}}$, and there are $C_{N_{\max}}^{N}$ possible cases that $q_i[u]$ can be reached to D_i successfully.

For the E node, IP of the message T_i in PRS-i can be exactly calculated as

$$\mathrm{IP}_{\mathrm{T}i}^{\mathrm{PRS}-i} = \sum_{N=H}^{N_{\max}} C_{N_{\max}}^{N} \left(\theta_{\mathrm{T}i}^{\mathrm{PRS}-i}\right)^{N} \left(1-\theta_{\mathrm{T}i}^{\mathrm{PRS}-i}\right)^{N_{\max}-N}, \quad (45)$$

where $\theta_{\mathrm{E}i}^{\mathrm{PRS}-i}$ is calculated by (38) and (42).

$$\theta_{\mathrm{T}i}^{\mathrm{PRS}-i} \overset{\Delta\to+\infty}{\approx} 1-\frac{\lambda_{\mathrm{RD}_i}}{\Omega_{\mathrm{RD}}}\left[1-\left(\frac{\lambda_{\mathrm{RE}}}{\lambda_{\mathrm{RE}}+\lambda_{\mathrm{SE}}\omega_{4,\mathrm{th}}}\right)^{M}\right]\left[1-\left(\frac{\lambda_{\mathrm{JE}}}{\lambda_{\mathrm{JE}}+\lambda_{\mathrm{RE}}\omega_{5,\mathrm{th}}}\right)^{N}\right] - \frac{\lambda_{\mathrm{RD}_j}}{\Omega_{\mathrm{RD}}}\left[1-\left(\frac{\lambda_{\mathrm{RE}}}{\lambda_{\mathrm{RE}}+\lambda_{\mathrm{SE}}\omega_{7,\mathrm{th}}}\right)^{M}\right]\left[1-\left(\frac{\lambda_{\mathrm{JE}}}{\lambda_{\mathrm{JE}}+\lambda_{\mathrm{RE}}\omega_{8,\mathrm{th}}}\right)^{N}\right]. \quad (40)$$

$$\begin{aligned}\theta_{\mathrm{Di}}^{\mathrm{PRS}-2} &= \exp\left(-\lambda_{\mathrm{SR}}\omega_{2,\mathrm{th}}\right)\sum_{p=0}^{M}(-1)^{p}C_{M}^{p}\frac{(M+1)\,\lambda_{\mathrm{RD}_i}}{(p+1)\,\Omega_{\mathrm{RD}}}\exp\left(-(p+1)\,\Omega_{\mathrm{RD}}\omega_{1,\mathrm{th}}\right)\\ &+\left(\exp\left(-\lambda_{\mathrm{SR}}\omega_{1,\mathrm{th}}\right)-\exp\left(-\lambda_{\mathrm{SR}}\omega_{2,\mathrm{th}}\right)\right)\sum_{p=0}^{M}(-1)^{p}\frac{C_{M}^{p}\,(M+1)\,\lambda_{\mathrm{RD}_i}}{(p+1)\,\Omega_{\mathrm{RD}}}\exp\left(-(p+1)\,\Omega_{\mathrm{RD}}\omega_{3,\mathrm{th}}\right)\\ &+\exp\left(-\lambda_{\mathrm{SR}}\omega_{2,\mathrm{th}}\right)\left[\begin{array}{l}\sum_{p=0}^{M}(-1)^{p}\frac{C_{M}^{p}(M+1)\lambda_{\mathrm{RD}_j}}{\lambda_{\mathrm{RD}_j}+p\Omega_{\mathrm{RD}}}\left(\exp\left(-\lambda_{\mathrm{RD}_i}\omega_{2,\mathrm{th}}\right)-\exp\left(-(p+1)\,\Omega_{\mathrm{RD}}\omega_{2,\mathrm{th}}\right)\right)\\ +\sum_{p=0}^{M}(-1)^{p}C_{M}^{p}\frac{(M+1)\lambda_{\mathrm{RD}_j}}{(p+1)\Omega_{\mathrm{RD}}}\exp\left(-(p+1)\,\Omega_{\mathrm{RD}}\omega_{2,\mathrm{th}}\right).\end{array}\right]. \quad (41)\end{aligned}$$

$$\begin{aligned}\theta_{\mathrm{T}i}^{\mathrm{PRS}-2} &= \frac{\lambda_{\mathrm{RD}_1}}{\Omega_{\mathrm{RD}}}\left(\frac{\lambda_{\mathrm{RE}}}{\lambda_{\mathrm{RE}}+\lambda_{\mathrm{SE}}\omega_{4,\mathrm{th}}}\right)^{M}\exp\left(-\lambda_{\mathrm{SE}}\omega_{1,\mathrm{th}}\right)+\frac{\lambda_{\mathrm{RD}_1}}{\Omega_{\mathrm{RD}}}\left(\frac{\lambda_{\mathrm{RE}}}{\lambda_{\mathrm{RE}}+\lambda_{\mathrm{SE}}\omega_{7,\mathrm{th}}}\right)^{M}\exp\left(-\lambda_{\mathrm{SE}}\omega_{2,\mathrm{th}}\right)\\ &+\frac{\lambda_{\mathrm{RD}_1}}{\Omega_{\mathrm{RD}}}\left[1-\left(\frac{\lambda_{\mathrm{RE}}}{\lambda_{\mathrm{RE}}+\lambda_{\mathrm{SE}}\omega_{4,\mathrm{th}}}\right)^{M}\exp\left(-\lambda_{\mathrm{SE}}\omega_{1,\mathrm{th}}\right)\right]\exp\left(-\lambda_{\mathrm{SR}}\omega_{2,\mathrm{th}}\right)\left(\frac{\lambda_{\mathrm{JE}}}{\lambda_{\mathrm{JE}}+\lambda_{\mathrm{RE}}\omega_{5,\mathrm{th}}}\right)^{N}\exp\left(-\lambda_{\mathrm{RE}}\omega_{1,\mathrm{th}}\right)\\ &+\frac{\lambda_{\mathrm{RD}_1}}{\Omega_{\mathrm{RD}}}\left[1-\left(\frac{\lambda_{\mathrm{RE}}}{\lambda_{\mathrm{RE}}+\lambda_{\mathrm{SE}}\omega_{4,\mathrm{th}}}\right)^{M}\exp\left(-\lambda_{\mathrm{SE}}\omega_{1,\mathrm{th}}\right)\right]\left[\exp\left(-\lambda_{\mathrm{SR}}\omega_{1,\mathrm{th}}\right)-\exp\left(-\lambda_{\mathrm{SR}}\omega_{2,\mathrm{th}}\right)\right]\\ &\times\left(\frac{\lambda_{\mathrm{JE}}}{\lambda_{\mathrm{JE}}+\lambda_{\mathrm{RE}}\omega_{6,\mathrm{th}}}\right)^{N}\exp\left(-\lambda_{\mathrm{RE}}\omega_{3,\mathrm{th}}\right)\\ &+\frac{\lambda_{\mathrm{RD}_2}}{\Omega_{\mathrm{RD}}}\left[\left(\frac{\lambda_{\mathrm{RE}}}{\lambda_{\mathrm{RE}}+\lambda_{\mathrm{SE}}\omega_{4,\mathrm{th}}}\right)^{M}\exp\left(-\lambda_{\mathrm{SE}}\omega_{1,\mathrm{th}}\right)-\left(\frac{\lambda_{\mathrm{RE}}}{\lambda_{\mathrm{RE}}+\lambda_{\mathrm{SE}}\omega_{7,\mathrm{th}}}\right)^{M}\exp\left(-\lambda_{\mathrm{SE}}\omega_{2,\mathrm{th}}\right)\right]\\ &\times\exp\left(-\lambda_{\mathrm{SR}}\omega_{2,\mathrm{th}}\right)\left(\frac{\lambda_{\mathrm{JE}}}{\lambda_{\mathrm{JE}}+\lambda_{\mathrm{RE}}\omega_{8,\mathrm{th}}}\right)^{N}\exp\left(-\lambda_{\mathrm{RE}}\omega_{2,\mathrm{th}}\right)\\ &+\frac{\lambda_{\mathrm{RD}_2}}{\Omega_{\mathrm{RD}}}\left[1-\left(\frac{\lambda_{\mathrm{RE}}}{\lambda_{\mathrm{RE}}+\lambda_{\mathrm{SE}}\omega_{4,\mathrm{th}}}\right)^{M}\exp\left(-\lambda_{\mathrm{SE}}\omega_{1,\mathrm{th}}\right)\right]\exp\left(-\lambda_{\mathrm{SR}}\omega_{2,\mathrm{th}}\right)\left(\frac{\lambda_{\mathrm{JE}}}{\lambda_{\mathrm{JE}}+\lambda_{\mathrm{RE}}\omega_{8,\mathrm{th}}}\right)^{N}\exp\left(-\lambda_{\mathrm{RE}}\omega_{2,\mathrm{th}}\right). \quad (42)\end{aligned}$$

$$\theta_{\mathrm{T}i}^{\mathrm{PRS}-2} \overset{\Delta\to+\infty}{\approx} 1-\frac{\lambda_{\mathrm{RD}_i}}{\Omega_{\mathrm{RD}}}\left[1-\left(\frac{\lambda_{\mathrm{RE}}}{\lambda_{\mathrm{RE}}+\lambda_{\mathrm{SE}}\omega_{4,\mathrm{th}}}\right)^{M}\right]\left[1-\left(\frac{\lambda_{\mathrm{JE}}}{\lambda_{\mathrm{JE}}+\lambda_{\mathrm{RE}}\omega_{5,\mathrm{th}}}\right)^{N}\right] - \frac{\lambda_{\mathrm{RD}_j}}{\Omega_{\mathrm{RD}}}\left[1-\left(\frac{\lambda_{\mathrm{RE}}}{\lambda_{\mathrm{RE}}+\lambda_{\mathrm{SE}}\omega_{7,\mathrm{th}}}\right)^{M}\right]\left[1-\left(\frac{\lambda_{\mathrm{JE}}}{\lambda_{\mathrm{JE}}+\lambda_{\mathrm{RE}}\omega_{8,\mathrm{th}}}\right)^{N}\right]. \quad (43)$$

TABLE 1. Values of the system parameters are used in Figs. 2-15.

Notation	ξ	$\gamma_{\rm th}$	H	$x_{\rm R}$	$x_{\rm D2}$
Value	3	1	5	[0.1, 0.9]	[0.8, 1.2]
Notation	$N_{\max}$	M	N	α	μ
Value	[5,7]	[1,5]	[1,5]	[0.7, 0.95]	[0.5, 1]

In (45), because E can accumulate N ($H \leq N$) packets, the message T_i is intercepted. In addition, probability that E in PRS-i incorrectly receives the packet $q_i[u]$ is $1-\theta_{{\rm E}i}^{{\rm PRS-i}}$, and there are $C_{N_{\max}}^{N}$ possible cases that $q_i[u]$ can be reached to E successfully.

Remark 8: From (35), (38), (41) and (42), due to the symmetry, i.e., $d_{{\rm RD}_1} = d_{{\rm RD}_2}$ ($\lambda_{{\rm RD}_1} = \lambda_{{\rm RD}_2}$), it is straightforward that $\theta_{\rm D1}^{{\rm PRS}-i} = \theta_{\rm D2}^{{\rm PRS}-i}$ and $\theta_{\rm T1}^{{\rm PRS}-i} = \theta_{\rm T2}^{{\rm PRS}-i}$, which also leads to ${\rm OP}_{\rm D1}^{{\rm PRS}-i} = {\rm OP}_{\rm D2}^{{\rm PRS}-i}$ and ${\rm IP}_{\rm T1}^{{\rm PRS}-i} = {\rm IP}_{\rm T2}^{{\rm PRS}-i}$. This means that the proposed PRS-1 and PRS-2 methods can obtain the performance fairness for two destinations. Moreover, from (40), (43) and (45), it is straightforward that IP of PRS-1 and PRS-2 at high transmit SNR regimes is the same, and does not depend on Δ.

IV. SIMULATION RESULTS

Section 4 presents Monte-Carlo simulations to verify the exact closed-form expressions of OP and IP of the PRS-1 and PRS-2 protocols. Both simulation and theoretical results are obtained by using computer software MATLAB. In each simulation, the Rayleigh channel coefficients of the X-Y links are generated by $h_{\rm XY} = 1/\sqrt{2\lambda_{\rm XY}} \times ({\rm randn}(1,1) + {\rm j} \times {\rm randn}(1,1))$, where $({\rm X}, {\rm Y}) \in \{{\rm S}, {\rm R}_m, {\rm D}_1, {\rm D}_2, {\rm J}_n, {\rm E}\}$, and randn(1,1) is a MATLAB function generating Gaussian distributed pseudo-random numbers with zero-mean and unit variance. In addition, 10^6-10^7 trials are generated in each simulation so that the simulation results nicely converge to the theoretical ones which are presented by the derived expressions of OP and IP. As presented in Figs. 2-15, the simulation results verify the accuracy of the theoretical ones.

For illustration purpose only, all the nodes are placed into an Oxy plane, where S locates at (0,0), all the relays are at $(x_{\rm R}, 0)$, position of D_1 is (1,0), all the jammer nodes (J_n) are placed at (1,0), and the E node is at (0.5,0.5). To present that the distances between the relays and two destinations are not much different, the destination D_2 is placed around the destination D_1 with the position of $(x_{\rm D2}, 0)$. As $x_{\rm D2} = 1$, this means that two destinations have the same distance to the relays. Next, in all the simulations, the path-loss exponential (ξ) is fixed by 3, the outage threshold ($\gamma_{\rm th}$) is assigned by 1, and the required number of encoded packets (H) is set by 5 (see Table 1). In all the figures, we denote Sim as Monte-Carlo simulation results, and Theory (Exact or Asymptotic) as the analytical results derived in Section III.

Figure 2 presents the outage performance of PRS-1 and PRS-2 as a function of the transmit SNR (Δ) in dB with

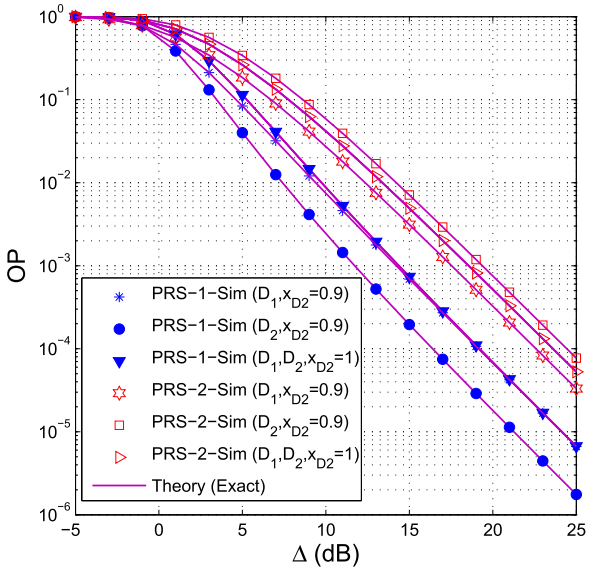

FIGURE 2. OP as a function of Δ (dB) when $M = 3$, $N = 3$, $x_{\rm R} = 0.5$, $\alpha = 0.85$, $\mu = 0.85$ and $N_{\max} = 6$.

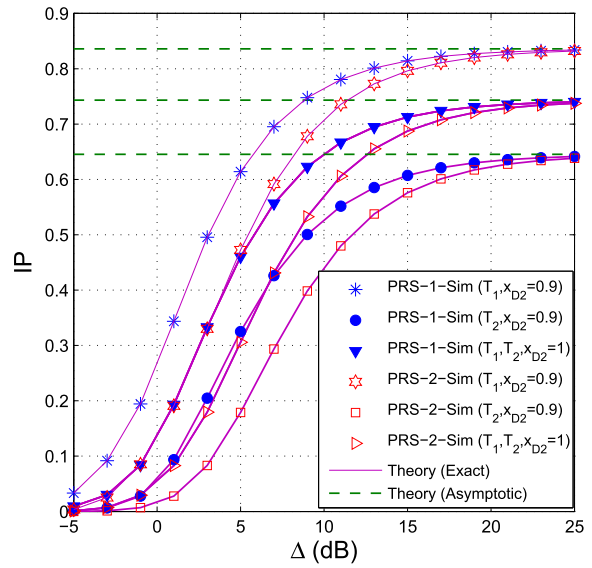

FIGURE 3. IP as a function of Δ (dB) when $M = 3$, $N = 3$, $x_{\rm R} = 0.5$, $\alpha = 0.85$, $\mu = 0.85$ and $N_{\max} = 6$.

different positions of D_2 when $M = N = 3$, $x_{\rm R} = 0.5$, $\alpha = \mu = 0.85$ and $N_{\max} = 6$. As we can see, as Δ increases (transmit power of the transmitters S and R_b increases), the OP values of both PRS-1 and PRS-2 rapidly decrease. It is also seen from Fig. 2 that the OP performance at the destinations in PRS-1 is better than those in PRS-2. In addition, when D_2 is at (0.9,0), D_2 in PRS-1 obtains lower OP than D_1, but in PRS-2, the OP performance of D_1 is better. When $x_{\rm D2} = 1$, we observe that OP of D_2 in PRS-i ($i = 1, 2$) is equal to that of D_1 (as stated in Remark 8) because the distances between two destinations to R_b are the same. Therefore, it is important to point out that the position of D_2 not only impacts on its OP but also impacts on OP of D_1.

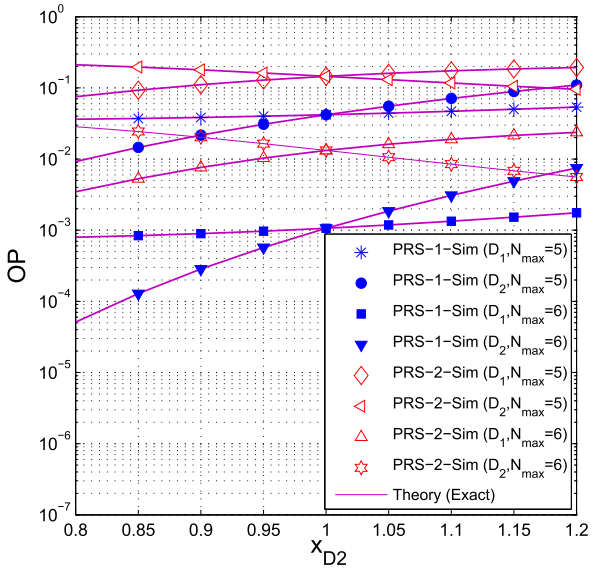

FIGURE 4. OP as a function of x_{D2} when $\Delta = 15$ dB, $M = 5$, $N = 2$, $x_R = 0.5$, $\alpha = 0.9$ and $\mu = 0.7$.

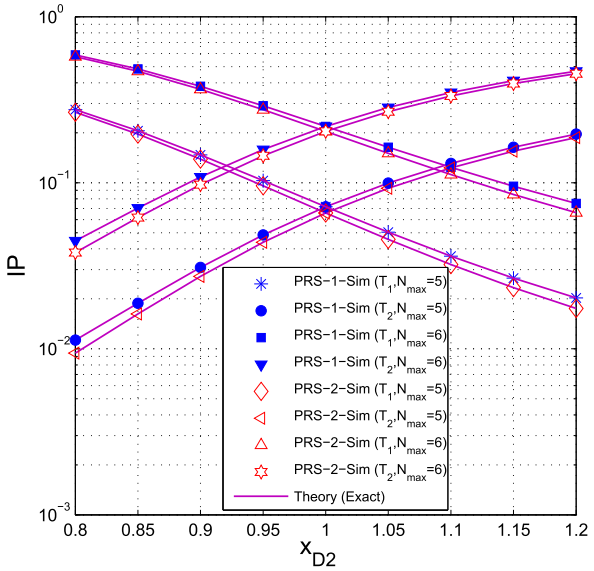

FIGURE 5. IP as a function of x_{D2} when $\Delta = 15$ dB, $M = 5$, $N = 2$, $x_R = 0.5$, $\alpha = 0.9$ and $\mu = 0.7$.

Figure 3 presents IP as a function of Δ in dB with the same system parameters as in Fig. 2 so that we can observe the trade-off between IP and OP. We first see that the IP values in PRS-1 and PRS-2 increase with the increasing of Δ, and at high Δ regions, they converge to the approximate results (as proved in Corollary 1 and Corollary 2). Next, it is shown that IP of the original data T_i ($i = 1, 2$) in PRS-1 is higher than the corresponding one in PRS-2. Moreover, when $x_{D2} = 0.9$, in both PRS-1 and PRS-2, IP of T_1 is higher than that of T_2. Similar to the OP performance, as $x_{D2} = 1$, IP of two messages T_1 and T_2 is the same.

From Figs. 2-3, it is interesting to find that as $x_{D2} = 1$, PRS-i provides the performance fairness between two destinations, in terms of OP and IP. In addition, there exists a trade-off between reliability and security, i.e., to obtain better OP performance, the transmit power of the source and relay nodes should be higher, however, the corresponding IP performance is worse. For another example, due to the lower IP performance, PRS-2 can be selected to deploy in the considered network, and the trade-off here is the OP-performance loss, as compared with PRS-1. Moreover, the obtained results in Figs. 2 and 3 can be used to optimally adjust the transmit power of the source and the selected relay. For example, we consider a wireless system using PRS-1, in which $x_{D2} = 0.9$ and quality of service (QoS) is that OP at two destinations must be below 0.01. From Figs. 2-3, we can see that the minimum value of Δ is about 10 dB so that the desired QoS is guaranteed and the IP value is minimum. It is worth noting that minimizing the transmit power means enhancing energy efficiency for the considered system.

In Figs. 4-5, we present the OP and IP performance as a function of x_{D2}, respectively, when $\Delta = 15$ dB, $M = 5$, $N = 2$, $x_R = 0.5$, $\alpha = 0.9$ and $\mu = 0.7$. As shown in Figs. 4-5, we can see that the position of D_2 also impacts on OP and IP of PRS-1 and PRS-2. Again, it is seen that the OP performance of PRS-1 is better than that of PRS-2, but the IP performance of PRS-1 is worse. In addition, when N_{max} increases, PRS-1 and PRS-2 obtain better OP performance, but their IP performance is worse. It is due to the fact that the D_1, D_2 and E nodes have more opportunity to collect enough encoded packets as the number of transmission times at the source increases. Also, as $x_{D2} = 1$, two destinations in PRS-1 and PRS-2 receive the same OP and IP values. It is worth noting from Figs. 4-5 that the performance gaps between two destinations increase as the difference between the d_{RD_1} and d_{RD_2} distances increases (or $|1 - x_{D2}|$ increases). Similar to Figs. 2-3, we also give an example of using the obtained results to design the system. Considering the system whose QoS has to be satisfied that OP of the D_1 and D_2 destination must be below 0.01, and IP of the T_1 and T_2 messages must be below 0.3. From Figs. 4-5, we can observe that only the OP and IP performance of PRS-1 satisfy the required QoS when the value of N_{max} is 6 and the position of D_2 is constrained by $0.95 \leq x_{D2} \leq 1.05$.

Figures 6 and 7 respectively present the OP and IP performance of PRS-i as a function of x_R, with different values of M (i.e., $M = 1, 4$). The remaining system parameters are fixed as follows: $\Delta = 7.5$ dB, $N = 2$, $x_{D2} = 1$, $\alpha = 0.8$, $\mu = 0.75$ and $N_{max} = 6$. Because $x_{D2} = 1$, the OP and IP performance of two the destinations in PRS-i are the same. As observed in Figs. 6-7, the position of the relays significantly impacts on the OP and IP values. Particularly, in Fig. 6, OP in PRS-1 is much lower than that in PRS-2 as the relays are near the destinations (x_R is high). On the contrary, PRS-2 obtains better OP performance as the source-relay distances are short (x_R is low). It is due to the fact that when x_R is high, the data transmission at two hops

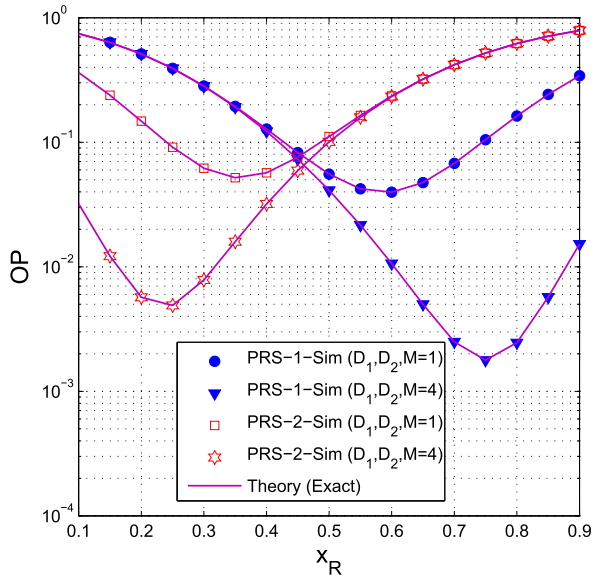

FIGURE 6. OP as a function of x_R when $\Delta = 7.5$ dB, $N = 2$, $x_{D2} = 1$, $\alpha = 0.8$, $\mu = 0.75$ and $N_{max} = 6$.

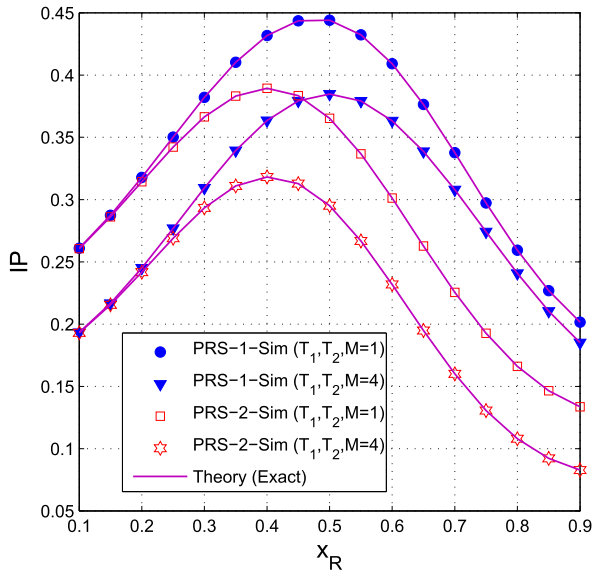

FIGURE 7. IP as a function of x_R when $\Delta = 7.5$ dB, $N = 2$, $x_{D2} = 1$, $\alpha = 0.8$, $\mu = 0.75$ and $N_{max} = 6$.

in PRS-1 is reliable, i.e., the channel quality of the first hop is enhanced by the relay selection, and that of the second hop is also better due to the short distances between the selected relay and two destinations. On the contrary, with high x_R values, the data transmission at the first hop in PRS-2 is less reliable due to the far distance between the source and the selected relay, which hence decreases the OP performance of PRS-2. Next, as x_R changes from 0.1 to 0.9, there exist optimal positions at which OP of PRS-i is lowest. For example, with $M = 1$, the OP performance of PRS-1 and PRS-2 is best when $x_R = 0.6$ and $x_R = 0.35$, respectively. Also seen from Fig. 6, the OP performance can be significantly improved by increasing the number of

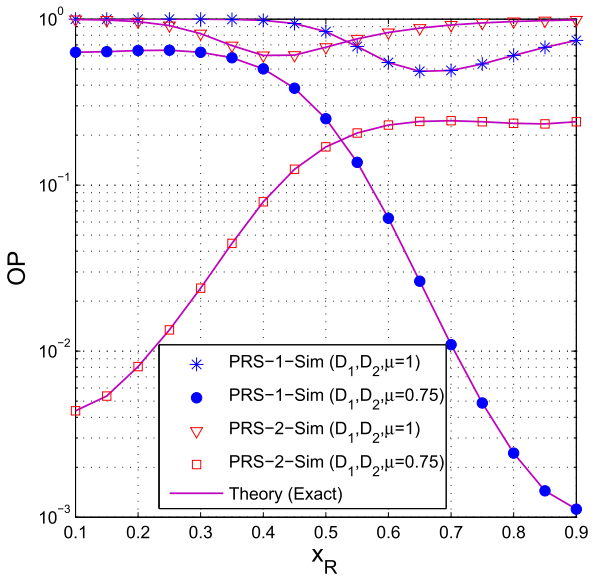

FIGURE 8. OP as a function of x_R when IP = 0.25, $M = 5$, $N = 1$, $x_{D2} = 1$, $\alpha = 0.8$ and $N_{max} = 6$.

relays. However, when the relays are very near the source (destinations), the OP values in PRS-1 (PRS-2) are the same, regardless of the value of M. In Fig. 7, we can see that the IP performance of PRS-2 is better than that of PRS-1. In addition, when $x_R \in \{0.4, 0.6\}$, the IP values are too high. It is due to the fact that at these positions, the distances between the relays and the eavesdropper are short, which improves quality of the relay-eavesdropper channels.It is also found in Fig. 7 that IP of PRS-1 and PRS-2 is much lower as M equals to 4.

From Figs. 6-7, it is worth noting that both OP and IP performance can be enhanced by increasing the number of relays. Moreover, the position of the relays should be carefully designed to optimize the system performance. For example, if the desired OP must be lower than 0.01, then looking at Fig. 6, the appropriate positions of the relays are $0.2 \leq x_R \leq 0.3$ (in PRS-2 with $M = 4$), and $0.65 \leq x_R \leq 0.85$ (in PRS-1 with $M = 4$). Then, using the results in Fig. 7, it can be found that when $x_R = 0.85$ and $x_R = 0.2$, the corresponding IP values in PRS-1 and PRS-2 are respectively lowest.

Figure 8 compares the OP performance of PRS-1 and PRS-2 when the IP values of PRS-1 and PRS-2 are fixed by 0.25. The remaining parameters in Fig. 8 are fixed by $M = 5$, $N = 1$, $x_{D2} = 1$, $\alpha = 0.8$ and $N_{max} = 6$. In this figure, with each value of x_R, we solve the equations $IP_{Ti}^{PRS-i} = 0.25$ to find the values of Δ. Then, the obtained values of Δ are used to calculate OP of PRS-1 and PRS-2. As shown in Fig. 8, PRS-1 obtains better OP performance when $x_R \geq 0.55$. When $\mu = 0.75$, it can be seen that the OP performance of PRS-1 (PRS-2) is best when x_R is highest (lowest). When CJ is not employed (denoted by Non-CJ), i.e., $\mu = 1$, the OP values of PRS-1 and PRS-2 are too high. It is due to the fact that without using CJ, the intercept possibility of the eavesdropper

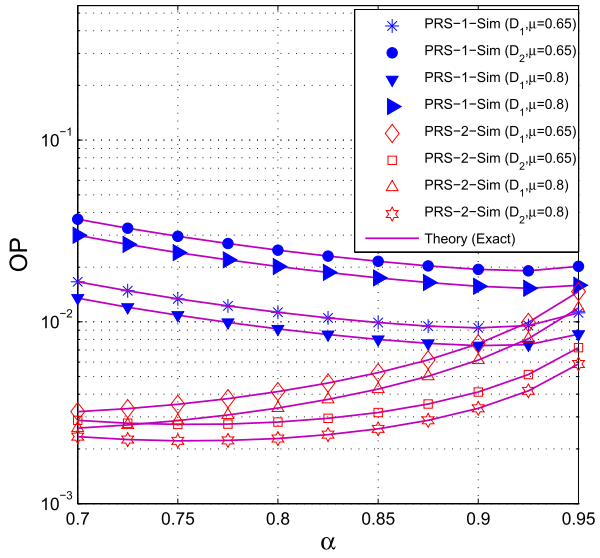

FIGURE 9. OP as a function of α when $\Delta = 25$ dB, $M = 5$, $N = 3$, $x_{D2} = 1.2$, $x_R = 0.35$ and $N_{max} = 5$.

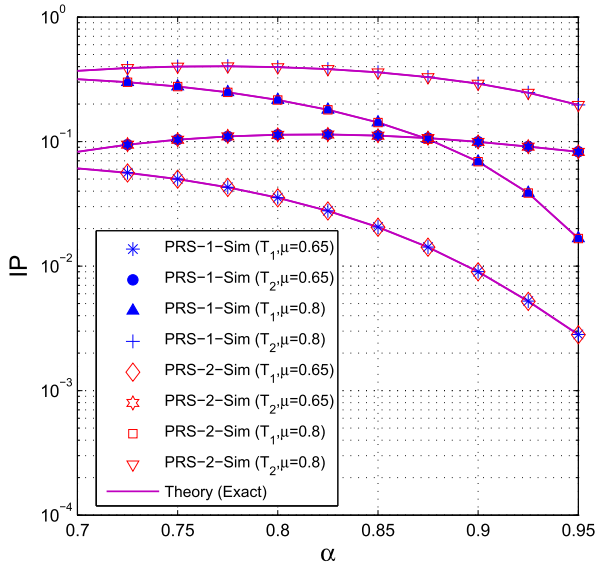

FIGURE 10. IP as a function of α when $\Delta = 25$ dB, $M = 5$, $N = 3$, $x_{D2} = 1.2$, $x_R = 0.35$ and $N_{max} = 5$.

is enhanced. Therefore, to obtain IP = 0.25, the transmitters in Non-CJ (including the source and the selected relay) have to reduce their transmit power significantly, which increases the OP values of PRS-1 and PRS-2.

From Figs. 6-8, we can see that the position of the relays can be used to determine that the PRS-1 protocol or the PRS2 protocol is better. In practice, PRS-1 or PRS-2 can be selected, relying on the specific positions of the relays.

In Figs. 9-10, we investigate impact of the power split factor α on the OP and IP performance, respectively, when $\Delta = 25$ dB, $M = 5$, $N = 3$, $x_{D2} = 1.2$, $x_R = 0.35$ and $N_{max} = 5$. Firstly, recalling (37); with $\gamma_{th} = 1$, we have $\alpha > 2/3$. This is the reason why the value of α only changes from 0.7 to 0.95 as presented in Figs. 9-10. Figure 9 shows

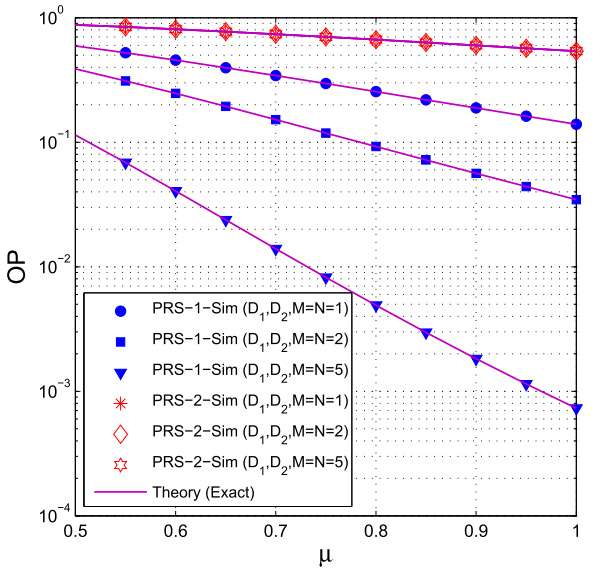

FIGURE 11. OP as a function of μ when $\Delta = 5$ dB, $x_{D2} = 1$, $x_R = 0.75$, $\alpha = 0.85$ and $N_{max} = 5$.

that the OP performance in PRS-1 and PRS-2 slightly changes as α varies. It is also seen that OP of PRS-2 is better than that of PRS-1 because the relays are near the source ($x_R = 0.35$). In PRS-1 (PRS-2), the OP performance of D_1 (D_2) is better that of D_2 (D_1). Moreover, as α increases, the OP values in PRS-1 decrease, but those in PRS-2 increase. Next, we can see that the OP performance of PRS-1 and PRS-2 is better, follows the increasing of μ, due to higher transmit power of the source and relay nodes.

In Fig. 10, we can see that the IP values of PRS-1 and PRS-2 at high transmit SNR ($\Delta = 25$ dB) are the same, which validates the derived expressions (40) and (43). It is also shown in Fig. 10 that the IP values of T_2 are lower than those of T_1 for all α. In addition, the IP performance is better with the lower value of μ because transmit power of the jammer nodes at the first and second hops is higher. From Figures 9 and 10, we again see the trade-off between OP and IP as changing the values of α and μ.

Figures 11 and 12 investigate impact of the factor μ on the OP and IP trade-off when $\Delta = 5$ dB, $x_{D2} = 1$, $x_R = 0.75$, $\alpha = 0.85$ and $N_{max} = 5$. In Fig. 11, the OP performance of PRS-1 is much better than that of PRS-2 because the relays are placed close to the destinations, i.e., $x_R = 0.75$. Moreover, similar to Fig. 6, it is again seen that the OP values in PRS-2 are the same for all values of M when x_R is high. For PRS-1, as expected, OP is lower with the increasing of M. Different with OP, the IP performance of PRS-1 is worse than that of PRS-2. We also observe from Fig. 12 that the number of the jammer nodes (M and N) also affects on IP. In particular, PRS-2 obtains lower IP as the values of M and N increase. However, the IP values in PRS-1 only change slightly with different values of M and N. Similar to Figs. 8-10, when the factor μ increases, the OP performance of the proposed protocols is better, but the IP performance is

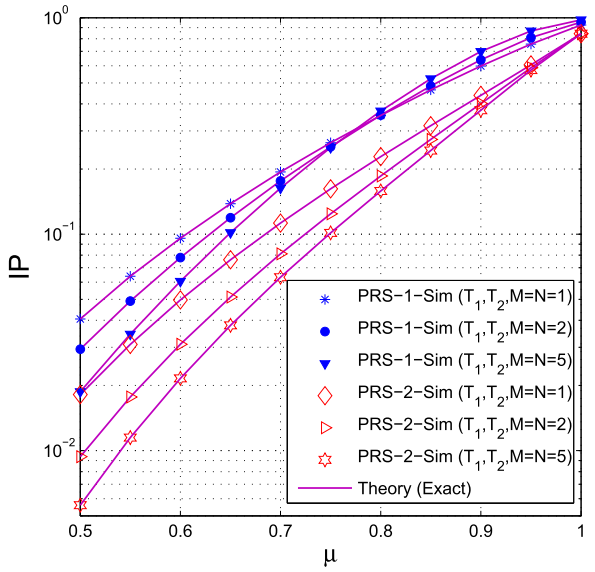

FIGURE 12. IP as a function of μ when $\Delta = 5$ dB, $x_{D2} = 1$, $x_R = 0.75$, $\alpha = 0.85$ and $N_{max} = 5$.

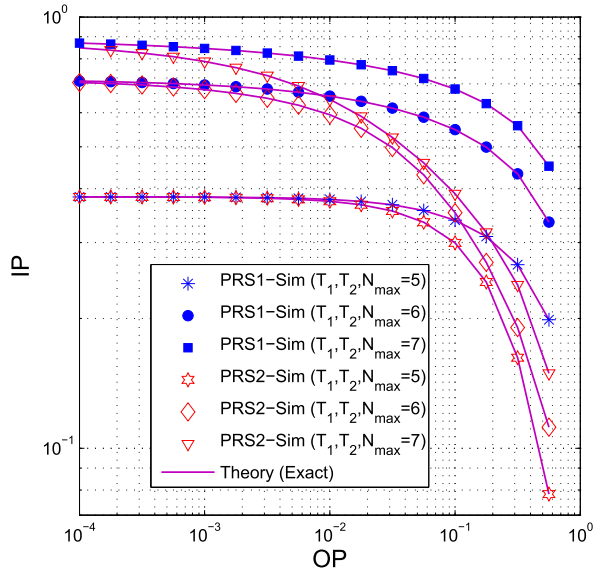

FIGURE 13. IP versus OP when $M = 5$, $N = 3$, $x_R = 0.4$, $x_{D2} = 1$, $\alpha = 0.85$ and $\mu = 0.85$.

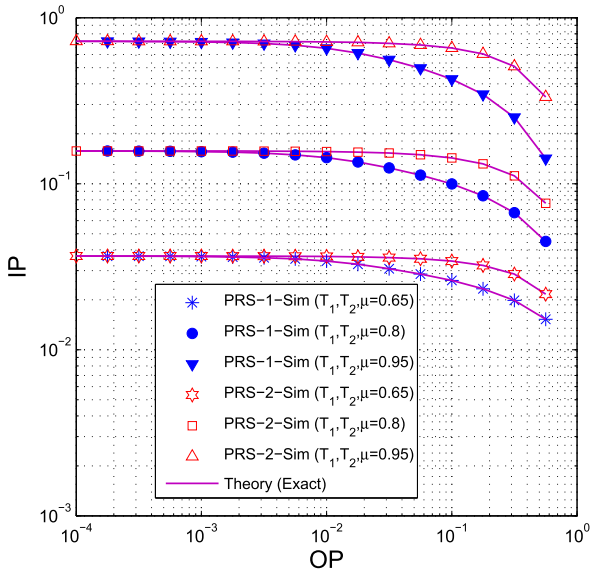

FIGURE 14. IP versus OP when $M = 3$, $N = 3$, $N_{max} = 5$, $x_{D2} = 1$, $\alpha = 0.9$ and $x_R = 0.65$.

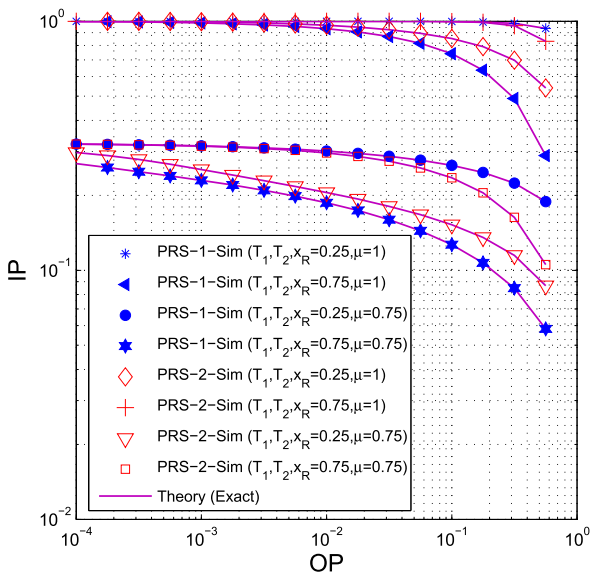

FIGURE 15. IP versus OP when $M = 4$, $N = 3$, $N_{max} = 6$, $x_{D2} = 1$, $\alpha = 0.85$ and $\mu = 0.75$.

degraded. As we can see, Non-CJ obtains the highest OP performance, however its IP performance is worst.

To show more clearly the SRT performance between PRS-1 and PRS-2, Figures 13-15 present IP as a function of OP. In particular, after setting up the system parameters (except Δ), we determine the target values of OP, and then solve equation $\mathrm{OP}_{Di}^{\mathrm{PRS}-i} = \mathrm{OP}$ to find the corresponding values of Δ. Then, the obtained Δ values are used to calculate the IP values. Therefore, the SRT performance is better if the obtained IP value is lower, at the same OP value. Moreover, for ease of observation and analysis, in Figs. 13-15, x_{D2} is fixed by 1 so that OP of two destinations (and IP of the original messages) is the same.

Figure 13 presents the SRT performance with various values of $N_{\max}$ when $M = 5$, $N = 3$, $x_R = 0.4$, $x_{D2} = 1$ and $\alpha = \mu = 0.85$. As shown in Fig. 13, to obtain lower target OP value, all the considered methods have to receive higher IP value. It is worth noting that when the target OP is very low, the transmit SNR Δ is high, and hence IP of PRS-1 and PRS-2 converges the asymptotic values. Figure 13 also shows that PRS-2 provides better SRT performance, and at medium and high target values of OP, IP of PRS-2 is much lower than that of PRS-1. Next, it is interesting to find that the SRT performance of PRS-i is degraded as $N_{\max}$ increases. As we can see, the SRT performance, with $N_{\max} = 5$, is much better than that with $N_{\max} = 6$ and 7.

Figure 14 investigates impact of μ on the SRT performance when $M = 3$, $N = 3$, $N_{\max} = 5$, $x_{\mathrm{D2}} = 1$, $\alpha = 0.9$ and $x_{\mathrm{R}} = 0.65$. It is seen that PRS-1 obtains better SRT performance as the relays are located at (0.65,0). Also in this figure, it is illustrated that the IP values of all the considered protocols significantly increases with the decreasing of μ. This also implies that the SRT performance can be enhanced by decreasing the transmit power of the transmitters and increasing that of the jammer nodes.

In Fig. 15, the SRT performance is presented with different positions of the relays, with and without using CJ ($\mu = 1$). The remaining parameters are fixed as $M = 4$, $N = 3$, $N_{\max} = 6$, $x_{\mathrm{D2}} = 1$, $\alpha = 0.85$ and $\mu = 0.75$. Observing the Non-CJ protocols, we see that their SRT performance is worst, and in addition, the IP values are almost equal to 1 at medium and low target OP regions. Figure 15 also presents that the position of the relays significantly impacts on the system performance, i.e., when $x_{\mathrm{R}} = 0.25$, PRS-2 obtains better SRT performance, but IP of PRS-1 is lower when $x_{\mathrm{R}} = 0.75$.

Therefore, from Figs. 13-15, we can see that the SRT performance of PRS-1 is better than that of PRS-2 when the relays are near the destinations, and vice verse.

V. CONCLUSION

In this paper, we proposed the RCs-based secure transmission protocol using NOMA, CJ and PRS to enhance the performance for dual-hop DF relaying networks, in terms of low complexity and latency, high reliability, throughput and security. The proposed protocol also obtained the performance fairness for two destinations via the adaptive power allocation method. We evaluated the OP and IP performance of the proposed protocol via both theory and simulations, which were always in the excellent agreement. The results presented that PRS-1 is better than PRS-2 when the relays are near the destinations, and vice verse. The obtained results also showed that the CJ technique plays a key role in the proposed protocol. In addition, the OP and IP performance can be significantly enhanced by optimally designed positions of the relays, transmit power allocated to the transmitter and jammer nodes, and number of the relays and jammers. For the OP-IP tradeoff, the SRT performance was better with lower transmit power, low number of transmission times of encoded packets and higher number of relays. Furthermore, our proposed protocols obtained much better SRT performance, as compared with the corresponding Non-CJ ones. In future, we will develop and analyze the proposed protocols over generalized fading channels such as Nakagami-*m*, Rician, etc.

APPENDIX A
PROOF OF THEOREM 1

Considering D_1; we note that in order that one encoded packet (i.e., $q_1[u]$) is successfully reached to D_1, R_b has to correctly decode it from S at the first time slot. Hence, probability of the successful decoding of one packet at D_1 can be formulated as in (A.1), as shown at the bottom of the page.

In (A.1), ρ_1 is the successfully decoding probability at D_1 in Case 1.1, i.e., both $q_1[u]$ and $q_2[u]$ are correctly obtained by R_b at the first time slot, and $q_1[u]$ is correctly received by D_1 at the second time slot. Substituting (19), (21) and (25) into (A.1), ρ_1 can be expressed under the following form:

$$\begin{aligned}\rho_1 &= \Pr\left(g_{\mathrm{SR}_b} \geq \omega_{1,\mathrm{th}}, g_{\mathrm{SR}_b} \geq \omega_{2,\mathrm{th}}\right) \\ &\quad \times \Pr\left(g_{\mathrm{R}_b\mathrm{D}_1} \leq g_{\mathrm{R}_b\mathrm{D}_2}, g_{\mathrm{R}_b\mathrm{D}_1} \geq \omega_{1,\mathrm{th}}\right) \\ &= \Pr\left(g_{\mathrm{SR}_b} \geq \omega_{2,\mathrm{th}}\right) \\ &\quad \times \Pr\left(g_{\mathrm{R}_b\mathrm{D}_1} \leq g_{\mathrm{R}_b\mathrm{D}_2}, g_{\mathrm{R}_b\mathrm{D}_1} \geq \omega_{1,\mathrm{th}}\right), \quad \text{(A.2)}\end{aligned}$$

where $\omega_{1,\mathrm{th}}$ and $\omega_{2,\mathrm{th}}$ are given by (36), and $0 < \omega_{1,\mathrm{th}} < \omega_{2,\mathrm{th}}$ (see (37)). Next, $\Pr\left(g_{\mathrm{SR}_b} \geq \omega_{2,\mathrm{th}}\right)$ in (A.2) can be exactly computed by using (4) as

$$\begin{aligned}\Pr\left(g_{\mathrm{SR}_b} \geq \omega_{2,\mathrm{th}}\right) &= 1 - F_{g_{\mathrm{SR}_b}}\left(\omega_{2,\mathrm{th}}\right) \\ &= 1 - \left(1 - \exp\left(-\lambda_{\mathrm{SR}}\omega_{2,\mathrm{th}}\right)\right)^{M+1}. \quad \text{(A.3)}\end{aligned}$$

For $\Pr\left(g_{\mathrm{R}_b\mathrm{D}_1} \leq g_{\mathrm{R}_b\mathrm{D}_2}, g_{\mathrm{R}_b\mathrm{D}_1} \geq \omega_{1,\mathrm{th}}\right)$ in (A.2), it can be further expressed as

$$\begin{aligned}&\Pr\left(g_{\mathrm{R}_b\mathrm{D}_1} \leq g_{\mathrm{R}_b\mathrm{D}_2}, g_{\mathrm{R}_b\mathrm{D}_1} \geq \omega_{1,\mathrm{th}}\right) \\ &\quad = \int_{\omega_{1,\mathrm{th}}}^{+\infty}\int_{x}^{+\infty} f_{g_{\mathrm{R}_b\mathrm{D}_1}}(x) f_{g_{\mathrm{R}_b\mathrm{D}_2}}(y)\, dydx. \quad \text{(A.4)}\end{aligned}$$

$$\begin{aligned}\theta_{\mathrm{D1}}^{\mathrm{PRS}-1} &= \underbrace{\Pr\left(g_{\mathrm{R}_b\mathrm{D}_1} \leq g_{\mathrm{R}_b\mathrm{D}_2}, \gamma_{\mathrm{SR}_b,x_1}^{\mathrm{C1}} \geq \gamma_{\mathrm{th}}, \gamma_{\mathrm{SR}_b,x_2}^{\mathrm{C1}} \geq \gamma_{\mathrm{th}}, \gamma_{\mathrm{R}_b\mathrm{D}_1,x_1}^{\mathrm{C1.1}} \geq \gamma_{\mathrm{th}}\right)}_{\rho_1} \\ &\quad + \underbrace{\Pr\left(g_{\mathrm{R}_b\mathrm{D}_1} \leq g_{\mathrm{R}_b\mathrm{D}_2}, \gamma_{\mathrm{SR}_b,x_1}^{\mathrm{C1}} \geq \gamma_{\mathrm{th}}, \gamma_{\mathrm{SR}_b,x_2}^{\mathrm{C1}} < \gamma_{\mathrm{th}}, \gamma_{\mathrm{R}_b\mathrm{D}_1,x_1}^{\mathrm{C1.2}} \geq \gamma_{\mathrm{th}}\right)}_{\rho_2} \\ &\quad + \underbrace{\Pr\left(g_{\mathrm{R}_b\mathrm{D}_1} > g_{\mathrm{R}_b\mathrm{D}_2}, \gamma_{\mathrm{SR}_b,x_2}^{\mathrm{C2}} \geq \gamma_{\mathrm{th}}, \gamma_{\mathrm{SR}_b,x_1}^{\mathrm{C2}} \geq \gamma_{\mathrm{th}}, \gamma_{\mathrm{R}_b\mathrm{D}_1,x_2}^{\mathrm{C2.1}} \geq \gamma_{\mathrm{th}}, \gamma_{\mathrm{R}_b\mathrm{D}_1,x_1}^{\mathrm{C2.1}} \geq \gamma_{\mathrm{th}}\right)}_{\rho_3}. \quad \text{(A.1)}\end{aligned}$$

Substituting PDFs of $g_{\mathrm{R}_b\mathrm{D}_1}$ and $g_{\mathrm{R}_b\mathrm{D}_2}$ into (A.4), after some manipulation, we obtain

$$\Pr\left(g_{\mathrm{R}_b\mathrm{D}_1} \le g_{\mathrm{R}_b\mathrm{D}_2}, g_{\mathrm{R}_b\mathrm{D}_1} \ge \omega_{1,\mathrm{th}}\right) = \frac{\lambda_{\mathrm{RD}_1}}{\Omega_{\mathrm{RD}}} \exp\left(-\Omega_{\mathrm{RD}}\omega_{1,\mathrm{th}}\right). \quad \text{(A.5)}$$

Next, ρ_2 in (A.1) refers to the event that D_1 correctly obtains $q_1[u]$ in Case 1.2, where only $q_1[u]$ is successfully received by R_b in the first time slot. We then rewrite ρ_2 as

$$\begin{aligned}\rho_2 &= \Pr\left(\omega_{1,\mathrm{th}} \le g_{\mathrm{SR}_b} < \omega_{2,\mathrm{th}}\right) \times \Pr\left(g_{\mathrm{R}_b\mathrm{D}_1} \le g_{\mathrm{R}_b\mathrm{D}_2}, g_{\mathrm{R}_b\mathrm{D}_1} \ge \omega_{3,\mathrm{th}}\right) \\ &= \left(F_{g_{\mathrm{SR}_b}}\left(\omega_{2,\mathrm{th}}\right) - F_{g_{\mathrm{SR}_b}}\left(\omega_{1,\mathrm{th}}\right)\right) \times \int_{\omega_{3,\mathrm{th}}}^{+\infty}\int_{x}^{+\infty} f_{g_{\mathrm{R}_b\mathrm{D}_1}}(x) f_{g_{\mathrm{R}_b\mathrm{D}_2}}(y)\, dydx,\end{aligned} \quad \text{(A.6)}$$

where $\omega_{3,\mathrm{th}}$ is given by (36). Then, after some algebraic calculation, we obtain (A.7), as shown at the bottom of the page.

As marked in (A.1), ρ_3 is the event that $q_1[u]$ is correctly reached to D_1 in Case 2, under the condition that both $q_1[u]$ and $q_2[u]$ are correctly obtained by R_b. Similar to the derivation of ρ_2, we can calculate ρ_3 as in (A.8), as shown at the bottom of the page.

Substituting (A.3), (A.5), (A.7) and (A.8) into (A.1), we then have the formula of $\theta_{\mathrm{D1}}^{\mathrm{PRS}-1}$. Furthermore, by replacing λ_{RD_1} and λ_{RD_2} in $\theta_{\mathrm{D1}}^{\mathrm{PRS}-1}$ by λ_{RD_2} and λ_{RD_1}, respectively, we can obtain the probability that D_2 can successfully obtain $q_2[u]$, denoted by $\theta_{\mathrm{D2}}^{\mathrm{PRS}-1}$. Finally, from $\theta_{\mathrm{D1}}^{\mathrm{PRS}-1}$ and $\theta_{\mathrm{D2}}^{\mathrm{PRS}-1}$, $\theta_{\mathrm{Di}}^{\mathrm{PRS}-1}$ can be expressed as in (35).

APPENDIX B
PROOF OF THEOREM 2

The probability that E correctly obtains $q_1[u]$ is formulated as in (B.1), as shown at the bottom of the page. Firstly, $\Pr\left(g_{\mathrm{R}_b\mathrm{D}_1} \le g_{\mathrm{R}_b\mathrm{D}_2}\right)$ and $\Pr\left(g_{\mathrm{R}_b\mathrm{D}_1} > g_{\mathrm{R}_b\mathrm{D}_2}\right)$ are respectively computed as

$$\begin{aligned}\Pr\left(g_{\mathrm{R}_b\mathrm{D}_1} \le g_{\mathrm{R}_b\mathrm{D}_2}\right) &= \int_0^{+\infty} f_{g_{\mathrm{R}_b\mathrm{D}_2}}(x)\, F_{g_{\mathrm{R}_b\mathrm{D}_1}}(x)\, dx \\ &= \frac{\lambda_{\mathrm{RD}_1}}{\Omega_{\mathrm{RD}}}, \\ \Pr\left(g_{\mathrm{R}_b\mathrm{D}_1} > g_{\mathrm{R}_b\mathrm{D}_2}\right) &= 1 - \Pr\left(g_{\mathrm{R}_b\mathrm{D}_1} \le g_{\mathrm{R}_b\mathrm{D}_2}\right) \\ &= \frac{\lambda_{\mathrm{RD}_2}}{\Omega_{\mathrm{RD}}}.\end{aligned} \quad \text{(B.2)}$$

$$\rho_2 = \left[\left(1 - \exp\left(-\lambda_{\mathrm{SR}}\omega_{2,\mathrm{th}}\right)\right)^{M+1} - \left(1 - \exp\left(-\lambda_{\mathrm{SR}}\omega_{1,\mathrm{th}}\right)\right)^{M+1}\right] \frac{\lambda_{\mathrm{RD}_1}}{\Omega_{\mathrm{RD}}} \exp\left(-\Omega_{\mathrm{RD}}\omega_{3,\mathrm{th}}\right). \quad \text{(A.7)}$$

$$\begin{aligned}\rho_3 &= \Pr\left(g_{\mathrm{SR}_b} \ge \omega_{1,\mathrm{th}}, g_{\mathrm{SR}_b} \ge \omega_{2,\mathrm{th}}\right) \Pr\left(g_{\mathrm{R}_b\mathrm{D}_1} > g_{\mathrm{R}_b\mathrm{D}_2}, g_{\mathrm{R}_b\mathrm{D}_1} \ge \omega_{1,\mathrm{th}}, g_{\mathrm{R}_b\mathrm{D}_1} \ge \omega_{2,\mathrm{th}}\right) \\ &= \Pr\left(g_{\mathrm{SR}_b} \ge \omega_{2,\mathrm{th}}\right) \Pr\left(g_{\mathrm{R}_b\mathrm{D}_1} > g_{\mathrm{R}_b\mathrm{D}_2}, g_{\mathrm{R}_b\mathrm{D}_1} \ge \omega_{2,\mathrm{th}}\right) \\ &= \left(1 - F_{g_{\mathrm{SR}_b}}\left(\omega_{2,\mathrm{th}}\right)\right) \int_{\omega_{2,\mathrm{th}}}^{+\infty}\int_{0}^{x} f_{g_{\mathrm{R}_b\mathrm{D}_1}}(x) f_{g_{\mathrm{R}_b\mathrm{D}_2}}(y)\, dydx \\ &= \left[1 - \left(1 - \exp\left(-\lambda_{\mathrm{SR}}\omega_{2,\mathrm{th}}\right)\right)^{M+1}\right] \left(\exp\left(-\lambda_{\mathrm{RD}_1}\omega_{2,\mathrm{th}}\right) - \frac{\lambda_{\mathrm{RD}_1}}{\Omega_{\mathrm{RD}}} \exp\left(-\Omega_{\mathrm{RD}}\omega_{2,\mathrm{th}}\right)\right).\end{aligned} \quad \text{(A.8)}$$

$$\begin{aligned}\theta_{\mathrm{T1}}^{\mathrm{PRS}-1} &= \Pr\left(g_{\mathrm{R}_b\mathrm{D}_1} \le g_{\mathrm{R}_b\mathrm{D}_2}\right) \Pr\left(\gamma_{\mathrm{SE},x_1}^{\mathrm{C1}} \ge \gamma_{\mathrm{th}}\right) \\ &+ \Pr\left(g_{\mathrm{R}_b\mathrm{D}_1} \le g_{\mathrm{R}_b\mathrm{D}_2}\right) \underbrace{\Pr\left(\gamma_{\mathrm{SE},x_1}^{\mathrm{C1}} < \gamma_{\mathrm{th}}\right) \Pr\left(\gamma_{\mathrm{SR}_b,x_1}^{\mathrm{C1}} \ge \gamma_{\mathrm{th}}, \gamma_{\mathrm{SR}_b,x_2}^{\mathrm{C1}} \ge \gamma_{\mathrm{th}}\right) \Pr\left(\gamma_{\mathrm{R}_b\mathrm{E},x_1}^{\mathrm{C1.1}} \ge \gamma_{\mathrm{th}}\right)}_{\chi_1} \\ &+ \Pr\left(g_{\mathrm{R}_b\mathrm{D}_1} \le g_{\mathrm{R}_b\mathrm{D}_2}\right) \underbrace{\Pr\left(\gamma_{\mathrm{SE},x_1}^{\mathrm{C1}} < \gamma_{\mathrm{th}}\right) \Pr\left(\gamma_{\mathrm{SR}_b,x_1}^{\mathrm{C1}} \ge \gamma_{\mathrm{th}}, \gamma_{\mathrm{SR}_b,x_2}^{\mathrm{C1}} < \gamma_{\mathrm{th}}\right) \Pr\left(\gamma_{\mathrm{R}_b\mathrm{E},x_1}^{\mathrm{C1.2}} \ge \gamma_{\mathrm{th}}\right)}_{\chi_2} \\ &+ \Pr\left(g_{\mathrm{R}_b\mathrm{D}_1} > g_{\mathrm{R}_b\mathrm{D}_2}\right) \underbrace{\Pr\left(\gamma_{\mathrm{SE},x_2}^{\mathrm{C2}} \ge \gamma_{\mathrm{th}}, \gamma_{\mathrm{SE},x_1}^{\mathrm{C2}} \ge \gamma_{\mathrm{th}}\right)}_{\chi_3} \\ &+ \Pr\left(g_{\mathrm{R}_b\mathrm{D}_1} > g_{\mathrm{R}_b\mathrm{D}_2}\right) \underbrace{\Pr\left(\gamma_{\mathrm{SE},x_2}^{\mathrm{C2}} \ge \gamma_{\mathrm{th}}, \gamma_{\mathrm{SE},x_1}^{\mathrm{C2}} < \gamma_{\mathrm{th}}\right) \Pr\left(\gamma_{\mathrm{SR}_b,x_2}^{\mathrm{C2}} \ge \gamma_{\mathrm{th}}, \gamma_{\mathrm{SR}_b,x_1}^{\mathrm{C2}} \ge \gamma_{\mathrm{th}}\right) \Pr\left(\gamma_{\mathrm{R}_b\mathrm{E},x_1}^{\mathrm{C2.1}} \ge \gamma_{\mathrm{th}}\right)}_{\chi_4} \\ &+ \Pr\left(g_{\mathrm{R}_b\mathrm{D}_1} > g_{\mathrm{R}_b\mathrm{D}_2}\right) \underbrace{\Pr\left(\gamma_{\mathrm{SE},x_2}^{\mathrm{C2}} < \gamma_{\mathrm{th}}\right) \Pr\left(\gamma_{\mathrm{SR}_b,x_2}^{\mathrm{C2}} \ge \gamma_{\mathrm{th}}, \gamma_{\mathrm{SR}_b,x_1}^{\mathrm{C2}} \ge \gamma_{\mathrm{th}}\right) \Pr\left(\gamma_{\mathrm{R}_b\mathrm{E},x_2}^{\mathrm{C2.1}} \ge \gamma_{\mathrm{th}}, \gamma_{\mathrm{R}_b\mathrm{E},x_1}^{\mathrm{C2.1}} \ge \gamma_{\mathrm{th}}\right)}_{\chi_5}.\end{aligned} \quad \text{(B.1)}$$

In (B.1), $\Pr\left(\gamma_{\mathrm{SE},x_1}^{\mathrm{C1}} \geq \gamma_{\mathrm{th}}\right)$ is probability that E can correctly obtain $q_1[u]$ from S in Case 1, and we further obtain

$$\begin{aligned}
&\Pr\left(\gamma_{\mathrm{SE},x_1}^{\mathrm{C1}} \geq \gamma_{\mathrm{th}}\right) \\
&= \Pr\left(g_{\mathrm{SE}} \geq \omega_{4,\mathrm{th}} \sum_{m=1}^{M} g_{\mathrm{R}_m\mathrm{E}} + \omega_{1,\mathrm{th}}\right) \\
&= \int_0^{+\infty} \cdots \int_0^{+\infty} \left(1 - F_{g_{\mathrm{SE}}}\left(\omega_{4,\mathrm{th}} \sum_{m=1}^{M} x_m + \omega_{1,\mathrm{th}}\right)\right) \\
&\quad \times f_{g_{\mathrm{R}_1\mathrm{E}}}(x_1) \ldots f_{g_{\mathrm{R}_M\mathrm{E}}}(x_M)\, dx_1 \ldots dx_M \\
&= \left(\frac{\lambda_{\mathrm{RE}}}{\lambda_{\mathrm{RE}} + \lambda_{\mathrm{SE}}\omega_{4,\mathrm{th}}}\right)^M \exp\left(-\lambda_{\mathrm{SE}}\omega_{1,\mathrm{th}}\right), \qquad \text{(B.3)}
\end{aligned}$$

where $\omega_{4,\mathrm{th}}$ is given by (39).

As marked in (B.1), χ_1 refers to the event that $q_1[u]$ is intercepted by E in the second time slot. This means that E cannot obtain $q_1[u]$ from S in the first time slot, and we have

$$\begin{aligned}
\chi_1 &= \Pr\left(\gamma_{\mathrm{SE},x_1}^{\mathrm{C1}} < \gamma_{\mathrm{th}}\right) \Pr\left(\gamma_{\mathrm{SR}_b,x_1}^{\mathrm{C1}} \geq \gamma_{\mathrm{th}}, \gamma_{\mathrm{SR}_b,x_2}^{\mathrm{C1}} \geq \gamma_{\mathrm{th}}\right) \\
&\quad \times \Pr\left(\gamma_{\mathrm{R}_b\mathrm{E},x_1}^{\mathrm{C1.1}} \geq \gamma_{\mathrm{th}}\right) \\
&= \left(1 - \Pr\left(g_{\mathrm{SE}} \geq \omega_{4,\mathrm{th}} \sum_{m=1}^{M} g_{\mathrm{R}_m\mathrm{E}} + \omega_{1,\mathrm{th}}\right)\right) \\
&\quad \times \left(1 - \Pr\left(g_{\mathrm{SR}_b} < \omega_{2,\mathrm{th}}\right)\right) \\
&\quad \times \Pr\left(g_{\mathrm{R}_b\mathrm{E}} \geq \omega_{5,\mathrm{th}} \sum_{n=1}^{N} g_{\mathrm{J}_n\mathrm{E}} + \omega_{1,\mathrm{th}}\right), \qquad \text{(B.4)}
\end{aligned}$$

where $\omega_{5,\mathrm{th}}$ is given by (39). Similar to (B.3), we have

$$\begin{aligned}
\chi_1 &= \left[1 - \left(\frac{\lambda_{\mathrm{RE}}}{\lambda_{\mathrm{RE}} + \lambda_{\mathrm{SE}}\omega_{4,\mathrm{th}}}\right)^M \exp\left(-\lambda_{\mathrm{SE}}\omega_{1,\mathrm{th}}\right)\right] \\
&\quad \times \left[1 - \left(1 - \exp\left(-\lambda_{\mathrm{SR}}\omega_{2,\mathrm{th}}\right)\right)^{M+1}\right] \\
&\quad \times \left(\frac{\lambda_{\mathrm{JE}}}{\lambda_{\mathrm{JE}} + \lambda_{\mathrm{RE}}\omega_{5,\mathrm{th}}}\right)^N \exp\left(-\lambda_{\mathrm{RE}}\omega_{1,\mathrm{th}}\right). \qquad \text{(B.5)}
\end{aligned}$$

For χ_2 in (B.1), this is probability that E cannot obtain $q_1[u]$ from S, but it can obtain it from R_b in Case 1.2. Similarly, χ_2 can be calculated as in (B.6), as shown at the bottom of the page, where $\omega_{6,\mathrm{th}}$ is obtained by (39).

Next, we consider probability that E can correctly receive $q_1[u]$ from S in Case 2 (see χ_3 in (B.1)). In addition, χ_3 can be exactly computed by (B.7), as shown at the bottom of the page, where $\omega_{7,\mathrm{th}}$ is given by (39), and from (37), we have $\omega_{7,\mathrm{th}} > \omega_{4,\mathrm{th}}$.

Considering χ_4 in (B.1); where E only obtains $q_2[u]$ from S, and then correctly receives $q_1[u]$ from R_b. Having $q_2[u]$ in hand, E can remove the modulated signals of $q_2[u]$ from the signals received from R_b. Therefore, we can rewrite χ_4 as in (B.8), as shown at the bottom of the page, where $\omega_{8,\mathrm{th}}$ is given by (39), and $g_{\mathrm{RE,sum}} = \sum_{m=1}^{M} g_{\mathrm{R}_m\mathrm{E}}$. Moreover, since $g_{\mathrm{RE,sum}}$ is summation of the exponential RVs, its PDF can be expressed as in [10, eq. (A.2)]:

$$f_{g_{\mathrm{RE,sum}}}(v) = \frac{(\lambda_{\mathrm{RE}})^M}{(M-1)!} v^{M-1} \exp\left(-\lambda_{\mathrm{RE}} v\right). \qquad \text{(B.9)}$$

$$\begin{aligned}
\chi_2 &= \left(1 - \Pr\left(g_{\mathrm{SE}} \geq \omega_{4,\mathrm{th}} \sum_{m=1}^{M} g_{\mathrm{R}_m\mathrm{E}} + \omega_{1,\mathrm{th}}\right)\right) \Pr\left(\omega_{1,\mathrm{th}} < g_{\mathrm{SR}_b} \leq \omega_{2,\mathrm{th}}\right) \Pr\left(g_{\mathrm{R}_b\mathrm{E}} \geq \omega_{6,\mathrm{th}} \sum_{n=1}^{N} g_{\mathrm{J}_n\mathrm{E}} + \omega_{3,\mathrm{th}}\right) \\
&= \left[1 - \left(\frac{\lambda_{\mathrm{RE}}}{\lambda_{\mathrm{RE}} + \lambda_{\mathrm{SE}}\omega_{4,\mathrm{th}}}\right)^M \exp\left(-\lambda_{\mathrm{SE}}\omega_{1,\mathrm{th}}\right)\right] \left[\left(1 - \exp\left(-\lambda_{\mathrm{SR}}\omega_{2,\mathrm{th}}\right)\right)^{M+1} - \left(1 - \exp\left(-\lambda_{\mathrm{SR}}\omega_{1,\mathrm{th}}\right)\right)^{M+1}\right] \\
&\quad \times \left(\frac{\lambda_{\mathrm{JE}}}{\lambda_{\mathrm{JE}} + \lambda_{\mathrm{RE}}\omega_{6,\mathrm{th}}}\right)^N \exp\left(-\lambda_{\mathrm{RE}}\omega_{3,\mathrm{th}}\right). \qquad \text{(B.6)}
\end{aligned}$$

$$\begin{aligned}
\chi_3 &= \Pr\left(g_{\mathrm{SE}} \geq \omega_{4,\mathrm{th}} \sum_{m=1}^{M} g_{\mathrm{R}_m\mathrm{E}} + \omega_{1,\mathrm{th}}, g_{\mathrm{SE}} \geq \omega_{7,\mathrm{th}} \sum_{m=1}^{M} g_{\mathrm{R}_m\mathrm{E}} + \omega_{2,\mathrm{th}}\right) \\
&= \Pr\left(g_{\mathrm{SE}} \geq \omega_{7,\mathrm{th}} \sum_{m=1}^{M} g_{\mathrm{R}_m\mathrm{E}} + \omega_{2,\mathrm{th}}\right) \\
&= \frac{\lambda_{\mathrm{RD}_2}}{\Omega_{\mathrm{RD}}} \left(\frac{\lambda_{\mathrm{RE}}}{\lambda_{\mathrm{RE}} + \lambda_{\mathrm{SE}}\omega_{7,\mathrm{th}}}\right)^M \exp\left(-\lambda_{\mathrm{SE}}\omega_{2,\mathrm{th}}\right). \qquad \text{(B.7)}
\end{aligned}$$

$$\begin{aligned}
\chi_4 &= \underbrace{\Pr\left(\omega_{4,\mathrm{th}} g_{\mathrm{RE,sum}} + \omega_{1,\mathrm{th}} \leq g_{\mathrm{SE}} \leq \omega_{7,\mathrm{th}} g_{\mathrm{RE,sum}} + \omega_{2,\mathrm{th}}\right)}_{\chi_{4,1}} \left(1 - \Pr\left(g_{\mathrm{SR}_b} < \omega_{2,\mathrm{th}}\right)\right) \\
&\quad \times \Pr\left(g_{\mathrm{R}_b\mathrm{E}} \geq \omega_{8,\mathrm{th}} \sum_{n=1}^{N} g_{\mathrm{J}_n\mathrm{E}} + \omega_{2,\mathrm{th}}\right). \qquad \text{(B.8)}
\end{aligned}$$

Using (B.9), we can calculate $\chi_{4,1}$ in (B.8) as in (B.10), as shown at the bottom of the page. Then, the obtained results in (B.8) and (B.10), χ_4 is given as in (B.11), as shown at the bottom of the page.

Next, χ_5 in (B.1) is probability that E correctly receives $q_1[u]$ from R_b in Case 2.1 when E cannot decode both $q_2[u]$ and $q_1[u]$ from S. We then obtain χ_5 as in (B.12), as shown at the bottom of the page.

Substituting (B.2), (B.3), (B.5), (B.6), (B.7), (B.11) and (B.12) into (B.1), we obtain an exact closed-form formula of $\theta_{\mathrm{T1}}^{\mathrm{PRS}-1}$. With the same derivation technique, $\theta_{\mathrm{T1}}^{\mathrm{PRS}-2}$ is also obtained, and we then have the desired expression of $\theta_{\mathrm{T}i}^{\mathrm{PRS}-1}$ as shown in (38).

APPENDIX C
PROOF OF THEOREM 3

Similar to Appendix A, $\theta_{\mathrm{D1}}^{\mathrm{PRS}-2}$ can be formulated as

$$\begin{aligned}\theta_{\mathrm{D1}}^{\mathrm{PRS}-2} &= \Pr\left(g_{\mathrm{SR}_b} \geq \omega_{2,\mathrm{th}}\right) \\ &\quad \times \Pr\left(g_{\mathrm{R}_b\mathrm{D}_1} \leq g_{\mathrm{R}_b\mathrm{D}_2}, g_{\mathrm{R}_b\mathrm{D}_1} \geq \omega_{1,\mathrm{th}}\right) \\ &\quad + \Pr\left(\omega_{1,\mathrm{th}} \leq g_{\mathrm{SR}_b} < \omega_{2,\mathrm{th}}\right) \\ &\quad \times \Pr\left(g_{\mathrm{R}_b\mathrm{D}_1} \leq g_{\mathrm{R}_b\mathrm{D}_2}, g_{\mathrm{R}_b\mathrm{D}_1} \geq \omega_{3,\mathrm{th}}\right) \\ &\quad + \Pr\left(g_{\mathrm{SR}_b} \geq \omega_{2,\mathrm{th}}\right) \\ &\quad \times \Pr\left(g_{\mathrm{R}_b\mathrm{D}_1} > g_{\mathrm{R}_b\mathrm{D}_2}, g_{\mathrm{R}_b\mathrm{D}_1} \geq \omega_{2,\mathrm{th}}\right). \end{aligned} \tag{C.1}$$

Because PRS-2 uses CSIs at the second hop for the relay selection, g_{SR_b} is only an exponential RV. Hence, we have

$$\begin{aligned}\Pr\left(g_{\mathrm{SR}_b} \geq \omega_{2,\mathrm{th}}\right) &= 1 - F_{g_{\mathrm{SR}_b}}\left(\omega_{2,\mathrm{th}}\right) = \exp\left(-\lambda_{\mathrm{SR}}\omega_{2,\mathrm{th}}\right), \\ \Pr\left(\omega_{1,\mathrm{th}} \leq g_{\mathrm{SR}_b} < \omega_{2,\mathrm{th}}\right) &= F_{g_{\mathrm{SR}_b}}\left(\omega_{2,\mathrm{th}}\right) - F_{g_{\mathrm{SR}_b}}\left(\omega_{1,\mathrm{th}}\right) \\ &= \exp\left(-\lambda_{\mathrm{SR}}\omega_{1,\mathrm{th}}\right) - \exp\left(-\lambda_{\mathrm{SR}}\omega_{2,\mathrm{th}}\right). \end{aligned} \tag{C.2}$$

Next, considering $\Pr\left(g_{\mathrm{R}_b\mathrm{D}_1} \leq g_{\mathrm{R}_b\mathrm{D}_2}, g_{\mathrm{R}_b\mathrm{D}_1} \geq \omega_{1,\mathrm{th}}\right)$ in (C.1); we note that RVs $g_{\mathrm{R}_b\mathrm{D}_1}$ and $g_{\mathrm{R}_b\mathrm{D}_2}$ are not independent because they have the joint PDF $f_{\varphi_b}(x)$ given in (9). Hence, to calculate $\Pr\left(g_{\mathrm{R}_b\mathrm{D}_1} \leq g_{\mathrm{R}_b\mathrm{D}_2}, g_{\mathrm{R}_b\mathrm{D}_1} \geq \omega_{1,\mathrm{th}}\right)$, we have to apply the method proposed in [51], [52], [55], i.e.,

$$\begin{aligned}&\Pr\left(g_{\mathrm{R}_b\mathrm{D}_1} \leq g_{\mathrm{R}_b\mathrm{D}_2}, g_{\mathrm{R}_b\mathrm{D}_1} \geq \omega_{1,\mathrm{th}}\right) \\ &\qquad = \int_0^{+\infty} \frac{\partial Q_1(x)}{\partial x} \frac{f_{\varphi_b}(x)}{f_{\varphi_m}(x)} dx, \end{aligned} \tag{C.3}$$

where $Q_1(x)$ is given by (C.4), as shown at the bottom of the next page. Then, we have

$$\frac{\partial Q_1(x)}{\partial x} = \begin{cases} 0, & \text{if } x \leq \omega_{1,\mathrm{th}} \\ \lambda_{\mathrm{RD}_1} \exp\left(-\Omega_{\mathrm{RD}}x\right), & \text{if } x > \omega_{1,\mathrm{th}} \end{cases} \tag{C.5}$$

Substituting (C.5), (7) and (9) into (C.3), after some manipulation, which yields

$$\begin{aligned}&\Pr\left(g_{\mathrm{R}_b\mathrm{D}_1} \leq g_{\mathrm{R}_b\mathrm{D}_2}, g_{\mathrm{R}_b\mathrm{D}_1} \geq \omega_{1,\mathrm{th}}\right) \\ &= \sum_{p=0}^{M} (-1)^p C_M^p \frac{(M+1)\lambda_{\mathrm{RD}_1}}{(p+1)\Omega_{\mathrm{RD}}} \exp\left(-(p+1)\Omega_{\mathrm{RD}}\omega_{1,\mathrm{th}}\right). \end{aligned} \tag{C.6}$$

$$\begin{aligned}\chi_{4,1} &= \int_0^{+\infty} \left(F_{g_{\mathrm{SE}}}\left(\omega_{7,\mathrm{th}}x + \omega_{2,\mathrm{th}}\right) - F_{g_{\mathrm{SE}}}\left(\omega_{4,\mathrm{th}}x + \omega_{1,\mathrm{th}}\right)\right) f_{g_{\mathrm{RE,sum}}}(x)\, dx \\ &= \frac{(\lambda_{\mathrm{RE}})^M}{(M-1)!} \exp\left(-\lambda_{\mathrm{SE}}\omega_{1,\mathrm{th}}\right) \int_0^{+\infty} x^{M-1} \exp\left(-\left(\lambda_{\mathrm{RE}} + \lambda_{\mathrm{SE}}\omega_{4,\mathrm{th}}\right)x\right) dx \\ &\quad - \frac{(\lambda_{\mathrm{RE}})^M}{(M-1)!} \exp\left(-\lambda_{\mathrm{SE}}\omega_{2,\mathrm{th}}\right) \int_0^{+\infty} x^{M-1} \exp\left(-\left(\lambda_{\mathrm{RE}} + \lambda_{\mathrm{SE}}\omega_{7,\mathrm{th}}\right)x\right) dx \\ &= \left(\frac{\lambda_{\mathrm{RE}}}{\lambda_{\mathrm{RE}} + \lambda_{\mathrm{SE}}\omega_{4,\mathrm{th}}}\right)^M \exp\left(-\lambda_{\mathrm{SE}}\omega_{1,\mathrm{th}}\right) - \left(\frac{\lambda_{\mathrm{RE}}}{\lambda_{\mathrm{RE}} + \lambda_{\mathrm{SE}}\omega_{7,\mathrm{th}}}\right)^M \exp\left(-\lambda_{\mathrm{SE}}\omega_{2,\mathrm{th}}\right). \end{aligned} \tag{B.10}$$

$$\begin{aligned}\chi_4 &= \left[\left(\frac{\lambda_{\mathrm{RE}}}{\lambda_{\mathrm{RE}} + \lambda_{\mathrm{SE}}\omega_{4,\mathrm{th}}}\right)^M \exp\left(-\lambda_{\mathrm{SE}}\omega_{1,\mathrm{th}}\right) - \left(\frac{\lambda_{\mathrm{RE}}}{\lambda_{\mathrm{RE}} + \lambda_{\mathrm{SE}}\omega_{7,\mathrm{th}}}\right)^M \exp\left(-\lambda_{\mathrm{SE}}\omega_{2,\mathrm{th}}\right)\right] \\ &\quad \times \left[1 - \left(1 - \exp\left(-\lambda_{\mathrm{SR}}\omega_{2,\mathrm{th}}\right)\right)^{M+1}\right] \left(\frac{\lambda_{\mathrm{JE}}}{\lambda_{\mathrm{JE}} + \lambda_{\mathrm{RE}}\omega_{8,\mathrm{th}}}\right)^N \exp\left(-\lambda_{\mathrm{RE}}\omega_{2,\mathrm{th}}\right). \end{aligned} \tag{B.11}$$

$$\begin{aligned}\chi_5 &= \Pr\left(g_{\mathrm{SE}} < \omega_{4,\mathrm{th}} g_{\mathrm{RE,sum}} + \omega_{1,\mathrm{th}}\right) \Pr\left(g_{\mathrm{SR}_b} \geq \omega_{1,\mathrm{th}}, g_{\mathrm{SR}_b} \geq \omega_{2,\mathrm{th}}\right) \Pr\left(g_{\mathrm{R}_b\mathrm{E}} \geq \omega_{8,\mathrm{th}} \sum_{n=1}^{N} g_{\mathrm{J}_n\mathrm{E}} + \omega_{2,\mathrm{th}}\right) \\ &= \left[1 - \left(\frac{\lambda_{\mathrm{RE}}}{\lambda_{\mathrm{RE}} + \lambda_{\mathrm{SE}}\omega_{4,\mathrm{th}}}\right)^M \exp\left(-\lambda_{\mathrm{SE}}\omega_{1,\mathrm{th}}\right)\right] \left[1 - \left(1 - \exp\left(-\lambda_{\mathrm{SR}}\omega_{2,\mathrm{th}}\right)\right)^{M+1}\right] \\ &\quad \times \left(\frac{\lambda_{\mathrm{JE}}}{\lambda_{\mathrm{JE}} + \lambda_{\mathrm{RE}}\omega_{8,\mathrm{th}}}\right)^N \exp\left(-\lambda_{\mathrm{RE}}\omega_{2,\mathrm{th}}\right). \end{aligned} \tag{B.12}$$

Next, with the similar derivation steps, we also have

$$\Pr\left(g_{\mathrm{R}_b\mathrm{D}_1} \le g_{\mathrm{R}_b\mathrm{D}_2}, g_{\mathrm{R}_b\mathrm{D}_1} \ge \omega_{3,\mathrm{th}}\right) = \sum_{p=0}^{M} (-1)^p C_M^p \frac{(M+1)\,\lambda_{\mathrm{RD}_1}}{(p+1)\,\Omega_{\mathrm{RD}}} \exp\left(-(p+1)\,\Omega_{\mathrm{RD}}\omega_{3,\mathrm{th}}\right). \tag{C.7}$$

Similarly, $\Pr\left(g_{\mathrm{R}_b\mathrm{D}_1} > g_{\mathrm{R}_b\mathrm{D}_2}, g_{\mathrm{R}_b\mathrm{D}_1} \ge \omega_{2,\mathrm{th}}\right)$ in (C.1) can be rewritten as

$$\Pr\left(g_{\mathrm{R}_b\mathrm{D}_1} > g_{\mathrm{R}_b\mathrm{D}_2}, g_{\mathrm{R}_b\mathrm{D}_1} \ge \omega_{2,\mathrm{th}}\right) = \int_0^{+\infty} \frac{\partial Q_2(x)}{\partial x} \frac{f_{\varphi_b}(x)}{f_{\varphi_m}(x)} dx. \tag{C.8}$$

In (C.8), $Q_2(x)$ can be calculated exactly as in (C.9), as shown at the bottom of the page. Then, we have

$$\frac{\partial Q_2(x)}{\partial x} = \begin{cases} \lambda_{\mathrm{RD}_2} \exp\left(-\lambda_{\mathrm{RD}_1}\omega_{2,\mathrm{th}}\right) \exp\left(-\lambda_{\mathrm{RD}_2}x\right), & \text{if } x \le \omega_{2,\mathrm{th}} \\ \lambda_{\mathrm{RD}_2} \exp\left(-\Omega_{\mathrm{RD}}x\right), & \text{if } x > \omega_{2,\mathrm{th}} \end{cases} \tag{C.10}$$

Combining (C.8) and (C.10), after some algebraic calculation, $\Pr\left(g_{\mathrm{R}_b\mathrm{D}_1} > g_{\mathrm{R}_b\mathrm{D}_2}, g_{\mathrm{R}_b\mathrm{D}_1} \ge \omega_{2,\mathrm{th}}\right)$ can be exactly expressed as in (C.11), as shown at the bottom of the page.

Plugging (C.1), (C.2), (C.6), (C.7) and (C.11) together, we have an exact closed-form expression of $\theta_{\mathrm{D1}}^{\mathrm{PRS}-2}$. Similarly, $\theta_{\mathrm{D2}}^{\mathrm{PRS}-2}$ is also obtained, and we finally have (41).

APPENDIX D
PROOF OF THEOREM 4

Similar to the derivation of $\theta_{\mathrm{T}i}^{\mathrm{PRS}-1}$; $\theta_{\mathrm{T}i}^{\mathrm{PRS}-2}$ can be formulated as in (B.1). At first, our objective is to calculate $\Pr\left(g_{\mathrm{R}_b\mathrm{D}_1} \le g_{\mathrm{R}_b\mathrm{D}_2}\right)$ in (B.1) which can be formulated as

$$\Pr\left(g_{\mathrm{R}_b\mathrm{D}_1} \le g_{\mathrm{R}_b\mathrm{D}_2}\right) = \int_0^{+\infty} \frac{\partial Q_3(x)}{\partial x} \frac{f_{\varphi_b}(x)}{f_{\varphi_m}(x)} dx, \tag{D.1}$$

where

$$Q_3(x) = \Pr\left(g_{\mathrm{R}_m\mathrm{D}_1} < g_{\mathrm{R}_m\mathrm{D}_2}, \min\left(g_{\mathrm{R}_m\mathrm{D}_1}, g_{\mathrm{R}_m\mathrm{D}_2}\right) < x\right) = \frac{\lambda_{\mathrm{RD}_1}}{\Omega_{\mathrm{RD}}} - \frac{\lambda_{\mathrm{RD}_1}}{\Omega_{\mathrm{RD}}} \exp\left(-\Omega_{\mathrm{RD}}x\right), \tag{D.2}$$

and

$$\frac{\partial Q_3(x)}{\partial x} = \lambda_{\mathrm{RD}_1} \exp\left(-\Omega_{\mathrm{RD}}x\right). \tag{D.3}$$

Combining (D.1), (D.3), and $\sum_{p=0}^{M} (-1)^p C_M^p \frac{(M+1)}{(p+1)} = 1$, which yields

$$\Pr\left(g_{\mathrm{R}_b\mathrm{D}_1} \le g_{\mathrm{R}_b\mathrm{D}_2}\right) = \sum_{p=0}^{M} (-1)^p C_M^p \frac{(M+1)\,\lambda_{\mathrm{RD}_1}}{(p+1)\,\Omega_{\mathrm{RD}}} = \frac{\lambda_{\mathrm{RD}_1}}{\Omega_{\mathrm{RD}}}. \tag{D.4}$$

Similarly, we have $\Pr\left(g_{\mathrm{R}_b\mathrm{D}_1} > g_{\mathrm{R}_b\mathrm{D}_2}\right) = \lambda_{\mathrm{RD}_2}/\Omega_{\mathrm{RD}}$.

$$Q_1(x) = \Pr\left(g_{\mathrm{R}_m\mathrm{D}_1} \le g_{\mathrm{R}_m\mathrm{D}_2}, g_{\mathrm{R}_m\mathrm{D}_1} \ge \omega_{1,\mathrm{th}}, \min\left(g_{\mathrm{R}_m\mathrm{D}_1}, g_{\mathrm{R}_m\mathrm{D}_2}\right) < x\right) = \begin{cases} 0, & \text{if } x \le \omega_{1,\mathrm{th}} \\ \int_{\omega_{1,\mathrm{th}}}^{x} f_{g_{\mathrm{R}_m\mathrm{D}_1}}(y) \int_y^{+\infty} f_{g_{\mathrm{R}_m\mathrm{D}_2}}(z)\, dz dy, & \text{if } x > \omega_{1,\mathrm{th}} \end{cases}$$
$$= \begin{cases} 0, & \text{if } x \le \omega_{1,\mathrm{th}} \\ \frac{\lambda_{\mathrm{RD}_1}}{\Omega_{\mathrm{RD}}}\left(\exp\left(-\Omega_{\mathrm{RD}}\omega_{1,\mathrm{th}}\right) - \exp\left(-\Omega_{\mathrm{RD}}x\right)\right), & \text{if } x > \omega_{1,\mathrm{th}} \end{cases} \tag{C.4}$$

$$Q_2(x) = \Pr\left(g_{\mathrm{R}_m\mathrm{D}_1} > g_{\mathrm{R}_m\mathrm{D}_2}, g_{\mathrm{R}_m\mathrm{D}_1} \ge \omega_{2,\mathrm{th}}, \min\left(g_{\mathrm{R}_m\mathrm{D}_1}, g_{\mathrm{R}_m\mathrm{D}_2}\right) < x\right) = \begin{cases} \exp\left(-\lambda_{\mathrm{RD}_1}\omega_{2,\mathrm{th}}\right)\left(1 - \exp\left(-\lambda_{\mathrm{RD}_2}x\right)\right), & \text{if } x \le \omega_{2,\mathrm{th}} \\ \exp\left(-\lambda_{\mathrm{RD}_1}\omega_{2,\mathrm{th}}\right) - \frac{\lambda_{\mathrm{RD}_1}}{\Omega_{\mathrm{RD}}} \exp\left(-\Omega_{\mathrm{RD}}\omega_{2,\mathrm{th}}\right) - \frac{\lambda_{\mathrm{RD}_2}}{\Omega_{\mathrm{RD}}} \exp\left(-\Omega_{\mathrm{RD}}x\right), & \text{if } x > \omega_{2,\mathrm{th}} \end{cases} \tag{C.9}$$

$$\Pr\left(g_{\mathrm{R}_b\mathrm{D}_1} > g_{\mathrm{R}_b\mathrm{D}_2}, g_{\mathrm{R}_b\mathrm{D}_1} \ge \omega_{2,\mathrm{th}}\right) = \sum_{p=0}^{M} (-1)^p \frac{C_M^p\,(M+1)\,\lambda_{\mathrm{RD}_2}}{\lambda_{\mathrm{RD}_2} + p\Omega_{\mathrm{RD}}} \left(\exp\left(-\lambda_{\mathrm{RD}_1}\omega_{2,\mathrm{th}}\right) - \exp\left(-(p+1)\,\Omega_{\mathrm{RD}}\omega_{2,\mathrm{th}}\right)\right) + \sum_{p=0}^{M} (-1)^p C_M^p \frac{(M+1)\,\lambda_{\mathrm{RD}_2}}{(p+1)\,\Omega_{\mathrm{RD}}} \exp\left(-(p+1)\,\Omega_{\mathrm{RD}}\omega_{2,\mathrm{th}}\right). \tag{C.11}$$

$$\chi_4 = \left[\left(\frac{\lambda_{\mathrm{RE}}}{\lambda_{\mathrm{RE}}+\lambda_{\mathrm{SE}}\omega_{4,\mathrm{th}}}\right)^M \exp\left(-\lambda_{\mathrm{SE}}\omega_{1,\mathrm{th}}\right) - \left(\frac{\lambda_{\mathrm{RE}}}{\lambda_{\mathrm{RE}}+\lambda_{\mathrm{SE}}\omega_{7,\mathrm{th}}}\right)^M \exp\left(-\lambda_{\mathrm{SE}}\omega_{2,\mathrm{th}}\right)\right] \times \exp\left(-\lambda_{\mathrm{SR}}\omega_{2,\mathrm{th}}\right)\left(\frac{\lambda_{\mathrm{JE}}}{\lambda_{\mathrm{JE}}+\lambda_{\mathrm{RE}}\omega_{8,\mathrm{th}}}\right)^N \exp\left(-\lambda_{\mathrm{RE}}\omega_{2,\mathrm{th}}\right),$$

$$\chi_5 = \frac{\lambda_{\mathrm{RD}_2}}{\Omega_{\mathrm{RD}}}\left[1-\left(\frac{\lambda_{\mathrm{RE}}}{\lambda_{\mathrm{RE}}+\lambda_{\mathrm{SE}}\omega_{4,\mathrm{th}}}\right)^M \exp\left(-\lambda_{\mathrm{SE}}\omega_{1,\mathrm{th}}\right)\right]\exp\left(-\lambda_{\mathrm{SR}}\omega_{2,\mathrm{th}}\right) \times\left(\frac{\lambda_{\mathrm{JE}}}{\lambda_{\mathrm{JE}}+\lambda_{\mathrm{RE}}\omega_{8,\mathrm{th}}}\right)^N \exp\left(-\lambda_{\mathrm{RE}}\omega_{2,\mathrm{th}}\right). \quad \text{(D.7)}$$

Next, χ_1 and χ_2 in (B.1) are re-calculated in PRS-2 as

$$\chi_1 = \left[1-\left(\frac{\lambda_{\mathrm{RE}}}{\lambda_{\mathrm{RE}}+\lambda_{\mathrm{SE}}\omega_{4,\mathrm{th}}}\right)^M \exp\left(-\lambda_{\mathrm{SE}}\omega_{1,\mathrm{th}}\right)\right] \times \exp\left(-\lambda_{\mathrm{SR}}\omega_{2,\mathrm{th}}\right) \times\left(\frac{\lambda_{\mathrm{JE}}}{\lambda_{\mathrm{JE}}+\lambda_{\mathrm{RE}}\omega_{5,\mathrm{th}}}\right)^N \exp\left(-\lambda_{\mathrm{RE}}\omega_{1,\mathrm{th}}\right). \quad \text{(D.5)}$$

$$\chi_2 = \left[1-\left(\frac{\lambda_{\mathrm{RE}}}{\lambda_{\mathrm{RE}}+\lambda_{\mathrm{SE}}\omega_{4,\mathrm{th}}}\right)^M \exp\left(-\lambda_{\mathrm{SE}}\omega_{1,\mathrm{th}}\right)\right] \times \left(\exp\left(-\lambda_{\mathrm{SR}}\omega_{1,\mathrm{th}}\right) - \exp\left(-\lambda_{\mathrm{SR}}\omega_{2,\mathrm{th}}\right)\right) \times\left(\frac{\lambda_{\mathrm{JE}}}{\lambda_{\mathrm{JE}}+\lambda_{\mathrm{RE}}\omega_{6,\mathrm{th}}}\right)^N \exp\left(-\lambda_{\mathrm{RE}}\omega_{3,\mathrm{th}}\right). \quad \text{(D.6)}$$

Next, it is noted that χ_3 in PRS-1 and PRS-2 is the same. For χ_4 and χ_5 in (B.1), they are re-computed in PRS-2, respectively as in (D.7), as shown at the top of the page. From the results obtained, we have (42), and the proof is complete.

REFERENCES

[1] P. Fazio, M. Tropea, M. Voznak, and F. De Rango, "On packet marking and Markov modeling for IP traceback: A deep probabilistic and stochastic analysis," *Comput. Netw.*, vol. 182, Aug. 2020, Art. no. 107464.

[2] F. De Rango, M. Tropea, and P. Fazio, "Mitigating DoS attacks in IoT EDGE layer to preserve QoS topics and nodes' energy," in *Proc. IEEE Conf. Comput. Commun. Workshops (INFOCOM WKSHPS)*, Toronto, ON, Canada, Jul. 2020, pp. 1–6.

[3] F. De Rango, G. Potrino, M. Tropea, and P. Fazio, "Energy-aware dynamic Internet of Things security system based on elliptic curve cryptography and message queue telemetry transport protocol for mitigating replay attacks," *Pervas. Mobile Comput.*, vol. 61, Jan. 2020, Art. no. 101105.

[4] N.-P. Nguyen, H. Q. Ngo, T. Q. Duong, H. D. Tuan, and K. Tourki, "Secure massive MIMO with the artificial noise-aided downlink training," *IEEE J. Sel. Areas Commun.*, vol. 36, no. 4, pp. 802–816, Apr. 2018.

[5] B. M. ElHalawany, A. A. A. El-Banna, and K. Wu, "Physical-layer security and privacy for vehicle-to-everything," *IEEE Commun. Mag.*, vol. 57, no. 10, pp. 84–90, Oct. 2019.

[6] K. N. Le and V. W. Y. Tam, "Wireless secrecy under multivariate correlated Nakagami-*m* fading," *IEEE Access*, vol. 8, pp. 33223–33236, 2020.

[7] Z. Wei, C. Masouros, F. Liu, S. Chatzinotas, and B. Ottersten, "Energy- and cost-efficient physical layer security in the era of IoT: The role of interference," *IEEE Commun. Mag.*, vol. 58, no. 4, pp. 81–87, Apr. 2020.

[8] J. Mo, M. Tao, and Y. Liu, "Relay placement for physical layer security: A secure connection perspective," *IEEE Commun. Lett.*, vol. 16, no. 6, pp. 878–881, Jun. 2012.

[9] C. Cai, Y. Cai, W. Yang, and W. Yang, "Secure connectivity using randomize-and-forward strategy in cooperative wireless networks," *IEEE Commun. Lett.*, vol. 17, no. 7, pp. 1340–1343, Jul. 2013.

[10] T. T. Duy, T. Q. Duong, T. L. Thanh, and V. N. Q. Bao, "Secrecy performance analysis with relay selection methods under impact of co-channel interference," *IET Commun.*, vol. 9, no. 11, pp. 1427–1435, Jul. 2015.

[11] L. Fan, X. Lei, N. Yang, T. Q. Duong, and G. K. Karagiannidis, "Secure multiple amplify-and-forward relaying with cochannel interference," *IEEE J. Sel. Topics Signal Process.*, vol. 10, no. 8, pp. 1494–1505, Dec. 2016.

[12] Y. Huang, J. Wang, C. Zhong, T. Q. Duong, and G. K. Karagiannidis, "Secure transmission in cooperative relaying networks with multiple antennas," *IEEE Trans. Wireless Commun.*, vol. 15, no. 10, pp. 6843–6856, Oct. 2016.

[13] X. Zhang, D. Guo, and K. Guo, "Secure performance analysis for multi-pair AF relaying massive MIMO systems in Ricean channels," *IEEE Access*, vol. 6, pp. 57708–57720, 2018.

[14] T. X. Quach, H. Tran, E. Uhlemann, and M. T. Truc, "Secrecy performance of cooperative cognitive radio networks under joint secrecy outage and primary user interference constraints," *IEEE Access*, vol. 8, pp. 18442–18455, 2020.

[15] Y. Chen, T. Zhang, X. Qiao, H. Wu, and J. Zhang, "Secure cognitive MIMO wiretap networks with different antenna transmission schemes," *IEEE Access*, vol. 9, pp. 5779–5790, 2021.

[16] X. Jiang, C. Zhong, X. Chen, T. Q. Duong, T. A. Tsiftsis, and Z. Zhang, "Secrecy performance of wirelessly powered wiretap channels," *IEEE Trans. Commun.*, vol. 64, no. 9, pp. 3858–3871, Sep. 2016.

[17] V. N. Vo, D.-D. Tran, C. So-In, and H. Tran, "Secrecy performance analysis for fixed-gain energy harvesting in an Internet of Things with untrusted relays," *IEEE Access*, vol. 6, pp. 48247–48258, 2018.

[18] Y. Zou, B. Champagne, W.-P. Zhu, and L. Hanzo, "Relay-selection improves the security-reliability trade-off in cognitive radio systems," *IEEE Trans. Commun.*, vol. 63, no. 1, pp. 215–228, Jan. 2015.

[19] J. Zhu, Y. Zou, B. Champagne, W. P. Zhu, and L. Hanzo, "Security–reliability tradeoff analysis of multirelay-aided decode-and-forward cooperation systems," *IEEE Trans. Veh. Technol.*, vol. 65, no. 7, pp. 5825–5831, Jul. 2016.

[20] Y. Zou, J. Zhu, X. Li, and L. Hanzo, "Relay selection for wireless communications against eavesdropping: A security-reliability trade-off perspective," *IEEE Netw.*, vol. 30, no. 9, pp. 74–79, Sep./Oct. 2016.

[21] X. Lu and R. C. D. Lamare, "Opportunistic relaying and jamming based on secrecy-rate maximization for multiuser buffer-aided relay systems," *IEEE Trans. Veh. Technol.*, vol. 69, no. 12, pp. 15269–15283, Dec. 2020.

[22] Z. Abdullah, G. Chen, M. A. M. Abdullah, and J. A. Chambers, "Enhanced secrecy performance of multihop IoT networks with cooperative hybrid-duplex jamming," *IEEE Trans. Inf. Forensics Security*, vol. 16, pp. 161–172, 2021.

[23] V. N. Vo, T. G. Nguyen, C. So-In, and D.-B. Ha, "Secrecy performance analysis of energy harvesting wireless sensor networks with a friendly jammer," *IEEE Access*, vol. 5, pp. 25196–25206, 2017.

[24] J. Si, Z. Cheng, Z. Li, J. Cheng, H.-M. Wang, and N. Al-Dhahir, "Cooperative jamming for secure transmission with both active and passive eavesdroppers," *IEEE Trans. Commun.*, vol. 68, no. 9, pp. 5764–5777, Sep. 2020.

[25] H. Xing, K.-K. Wong, A. Nallanathan, and R. Zhang, "Wireless powered cooperative jamming for secrecy multi-AF relaying networks," *IEEE Trans. Wireless Commun.*, vol. 15, no. 12, pp. 7971–7984, Dec. 2016.

[26] T. M. Hoang, T. Q. Duong, N.-S. Vo, and C. Kundu, "Physical layer security in cooperative energy harvesting networks with a friendly jammer," *IEEE Wireless Commun. Lett.*, vol. 6, no. 2, pp. 174–177, Apr. 2017.
[27] X. Ding, T. Song, Y. Zou, and X. Chen, "Security-reliability tradeoff for friendly jammer assisted user-pair selection in the face of multiple eavesdroppers," *IEEE Access*, vol. 4, pp. 8386–8393, 2016.
[28] X. Ding, T. Song, Y. Zou, X. Chen, and L. Hanzo, "Security-reliability tradeoff analysis of artificial noise aided two-way opportunistic relay selection," *IEEE Trans. Veh. Technol.*, vol. 66, no. 5, pp. 3930–3941, May 2017.
[29] Z. Cao, X. Ji, J. Wang, S. Zhang, Y. Ji, and J. Wang, "Security-reliability tradeoff analysis for underlay cognitive two-way relay networks," *IEEE Trans. Wireless Commun.*, vol. 18, no. 12, pp. 6030–6042, Dec. 2019.
[30] B. Selim, M. S. Alam, J. V. C. Evangelista, G. Kaddoum, and B. L. Agba, "NOMA-based IoT networks: Impulsive noise effects and mitigation," *IEEE Commun. Mag.*, vol. 58, no. 11, pp. 69–75, Nov. 2020.
[31] H. Lei, J. Zhang, K. H. Park, P. Xu, Z. Zhang, G. Pan, and M. S. Alouini, "Secrecy outage of max–min TAS scheme in MIMO-NOMA systems," *IEEE Trans. Veh. Technol.*, vol. 67, no. 8, pp. 6981–6990, Aug. 2018.
[32] J. Chen, L. Yang, and M.-S. Alouini, "Physical layer security for cooperative NOMA systems," *IEEE Trans. Veh. Technol.*, vol. 67, no. 5, pp. 4645–4649, May 2018.
[33] H. Lei, Z. Yang, K.-H. Park, I. S. Ansari, Y. Guo, G. Pan, and M.-S. Alouini, "Secrecy outage analysis for cooperative NOMA systems with relay selection schemes," *IEEE Trans. Commun.*, vol. 67, no. 9, pp. 6282–6298, Sep. 2019.
[34] V. N. Vo, C. So-In, H. Tran, D.-D. Tran, S. Heng, P. Aimtongkham, and A.-N. Nguyen, "On security and throughput for energy harvesting untrusted relays in IoT systems using NOMA," *IEEE Access*, vol. 7, pp. 149341–149354, 2019.
[35] T. Le Anh and I. P. Hong, "Secrecy performance of a multi-NOMA-MIMO system in the UEH relaying network using the PSO algorithm," *IEEE Access*, vol. 9, pp. 2317–2331, 2021.
[36] K. Cao, B. Wang, H. Ding, L. Lv, J. Tian, and F. Gong, "On the security enhancement of uplink NOMA systems with jammer selection," *IEEE Trans. Commun.*, vol. 68, no. 9, pp. 5747–5763, Sep. 2020.
[37] V. N. Vo, C. So-In, D.-D. Tran, and H. Tran, "Optimal system performance in multihop energy harvesting WSNs using cooperative NOMA and friendly jammers," *IEEE Access*, vol. 7, pp. 125494–125510, 2019.
[38] K. Cao, B. Wang, H. Ding, L. Lv, R. Dong, T. Cheng, and F. Gong, "Improving physical layer security of uplink NOMA via energy harvesting jammers," *IEEE Trans. Inf. Forensics Security*, vol. 16, pp. 786–799, 2021.
[39] B. Li, X. Qi, K. Huang, Z. Fei, F. Zhou, and R. Q. Hu, "Security-reliability tradeoff analysis for cooperative NOMA in cognitive radio networks," *IEEE Trans. Commun.*, vol. 67, no. 1, pp. 83–96, Jan. 2019.
[40] H. Niu, M. Iwai, K. Sezaki, L. Sun, and Q. Du, "Exploiting fountain codes for secure wireless delivery," *IEEE Commun. Lett.*, vol. 18, no. 5, pp. 777–780, May 2014.
[41] L. Sun, P. Ren, Q. Du, and Y. Wang, "Fountain-coding aided strategy for secure cooperative transmission in industrial wireless sensor networks," *IEEE Trans. Ind. Informat.*, vol. 12, no. 1, pp. 291–300, Feb. 2016.
[42] A. S. Khan and I. Chatzigeorgiou, "Opportunistic relaying and random linear network coding for secure and reliable communication," *IEEE Trans. Wireless Commun.*, vol. 17, no. 1, pp. 223–234, Jan. 2018.
[43] S. Jain and R. Bose, "QVP-based relay selection to improve secrecy for rateless-codes in delay-constrained systems," *IET Commun.*, vol. 13, no. 1, pp. 26–35, Jan. 2019.
[44] S. Jain and R. Bose, "Rateless-code-based secure cooperative transmission scheme for industrial IoT," *IEEE Internet Things J.*, vol. 7, no. 7, pp. 6550–6565, Jul. 2020.
[45] S. Jain and R. Bose, "Secure cooperative transmission in rateless-coded environment using TAS and artificial noise," *IEEE Trans. Veh. Technol.*, vol. 68, no. 12, pp. 12416–12421, Dec. 2019.
[46] P. T. Tin, T. Nguyen, N. Sang, T. T. Duy, P. Tran, and M. Voznak, "Rateless codes-based secure communication employing transmit antenna selection and harvest-to-jam under joint effect of interference and hardware impairments," *Entropy*, vol. 21, no. 7, p. 700, Jul. 2019.
[47] D. Huang and L. Sun, "Secure communication based on fountain code and channel feedback," in *Proc. 11th Int. Conf. Wireless Commun. Signal Process. (WCSP)*, Xi'an, China, Oct. 2019, pp. 1–5.
[48] L. Sun and H. Xu, "Fountain-coding-based secure communications exploiting outage prediction and limited feedback," *IEEE Trans. Veh. Technol.*, vol. 68, no. 1, pp. 740–753, Jan. 2019.
[49] L. Sun, D. Huang, and A. Lee Swindlehurst, "Fountain-coding aided secure transmission with delay and content awareness," *IEEE Trans. Veh. Technol.*, vol. 69, no. 7, pp. 7992–7997, Jul. 2020.
[50] M. Abughalwa and M. O. Hasna, "A secrecy study of UAV based networks with fountain codes and FD jamming," *IEEE Commun. Lett.*, vol. 25, no. 6, pp. 1796–1800, Jun. 2021, doi: 10.1109/LCOMM.2021.3056389.
[51] K. Tourki, H.-C. Yang, and M.-S. Alouini, "Accurate outage analysis of incremental decode-and-forward opportunistic relaying," *IEEE Trans. Wireless Commun.*, vol. 10, no. 4, pp. 1021–1025, Apr. 2011.
[52] K. Tourki, K. A. Qaraqe, and M.-S. Alouini, "Outage analysis for underlay cognitive networks using incremental regenerative relaying," *IEEE Trans. Veh. Technol.*, vol. 62, no. 2, pp. 721–734, Feb. 2013.
[53] D. T. Hung, T. T. Duy, P. T. Tran, D. Q. Trinh, and T. Hanh, "Performance comparison between fountain codes-based secure MIMO protocols with and without using non-orthogonal multiple access," *Entropy*, vol. 21, no. 10, p. 982, Oct. 2019.
[54] T. T. Duy, L. C. Khan, N. T. Binh, and N. L. Nhat, "Intercept probability analysis of cooperative cognitive networks using fountain codes and cooperative jamming," *EAI Trans. Ind. Netw. Intell. Syst.*, vol. 8, no. 26, pp. 1–9, Apr. 2021.
[55] T. T. Duy, T. Q. Duong, D. B. da Costa, V. N. Q. Bao, and M. Elkashlan, "Proactive relay selection with joint impact of hardware impairment and co-channel interference," *IEEE Trans. Commun.*, vol. 63, no. 5, pp. 1594–1606, May 2015.

DUY-HUNG HA was born in Binh Dinh, Vietnam, in 1977. He received the B.S. degree in electronics and telecommunications engineering from the Posts and Telecommunications Institute of Technology, Vietnam, in 2007, and the M.S. degree in electronics and telecommunications engineering from the University of Transport and Communications, Hanoi, Vietnam, in 2014. He is currently pursuing the Ph.D. degree in electrical engineering with the VSB—Technical University of Ostrava, Czech Republic. In 2017, he joined the Faculty of Electrical and Electronics Engineering, Ton Duc Thang University, Vietnam, as a Lecturer. His major research interests include cooperative communications, cognitive radio, and physical layer security.

TRAN TRUNG DUY (Member, IEEE) received the B.E. degree in electronics and telecommunications engineering from French-Vietnamese Training Program for Excellent Engineers (PFIEV), Ho Chi Minh City University of Technology, Vietnam, in 2007, and the Ph.D. degree in electrical engineering from the University of Ulsan, South Korea, in 2013. In 2013, he joined the Posts and Telecommunications Institute of Technology (PTIT), Ho Chi Minh City campus, as a Lecturer and a Researcher. His major research interests include cooperative communications, cooperative multi-hop, cognitive radio, physical-layer security, energy harvesting, hardware impairments, and fountain codes. He has been a member of the Technical Program Committee of conferences, such as SigTelCom, ComManTel, ATC, NICS, ISCE, and ICACCI. He received the prestigious 'Exemplary Reviewer' Certificates of IEEE Communications Letters, in 2016 and 2017, and the IEEE Transactions on Communications, in 2016. He served as an Associate Editor for *EAI Endorsed Transactions on Industrial Networks and Intelligent Systems* (EAI-INIS) journal and *REV Journal on Electronics and Communications* (REV-JEC) journal, in 2017, and *Hindawi Wireless Communications and Mobile Computing* (WCMC) journal and *Frontiers in Communications and Networks* journal, in 2021.

PHAM NGOC SON received the B.E. degree in electronics and telecommunications engineering from the Post and Telecommunication Institute of Technology, Ho Chi Minh City, in 2005, the M.E. degree in electronics and telecommunications engineering from Ho Chi Minh City University of Technology, Vietnam, in 2009, and the Ph.D. degree in electrical engineering from the University of Ulsan, South Korea, in 2015. He is currently a Lecturer with the Faculty of Electrical and Electronics Engineering, Ho Chi Minh City University of Technology and Education (HCMUTE). His major research interests include cooperative communication, cognitive radio, physical layer security, energy harvesting, full duplex transmission, non-orthogonal multiple access (NOMA), intelligent reflecting surface, and short packet communications.

THUONG LE-TIEN (Member, IEEE) was born in Saigon, Ho Chi Minh City, Vietnam. He received the bachelor's and master's degrees in electronics engineering from Ho Chi Minh City University of Technology (HCMUT), Vietnam, and the Ph.D. degree in telecommunications engineering from the University of Tasmania, Australia. Since May 1981, he has been with the Department of Electrical and Electronics Engineering, HCMUT. He spent three years at Ruhr Universität Bochum, Germany, as a Visiting Scholar, from 1989 to 1992. He served as the Deputy Department Head for many years and the Telecommunications Department Head, from 1998 to 2002. He had also appointed for the second position as the Director of Center for Overseas Studies, from 1998 to May 2010. He is currently a Full Professor at HCMUT. He has published more than 190 scientific articles and the teaching materials for university students related to electronic circuits one and two, digital signal processing and wavelets, antenna and wave propagation, and communication systems. His research interests include communication systems, signal processing, and electronic circuits.

MIROSLAV VOZNAK (Senior Member, IEEE) received the Ph.D. degree in telecommunications engineering from the Faculty of Electrical Engineering and Computer Science, VSB—Technical University of Ostrava, in 2002, and the Habilitation degree, in 2009. He was appointed as a Full Professor in electronics and communications technologies, in 2017. He has authored and coauthored over 100 articles indexed in SCI/SCIE journals. His research interests include information and communication technologies, especially on quality of service and experience, network security, wireless networks, and big data analytics. According to Stanford University study released in 2020, he is one of the World's Top 2% of scientists in networking and telecommunications and information and communications technologies.